Supporting Information

2D NMR-spectroscopic screening reveals polyketides in ladybugs

Stephen T. Deyrup, Laura E. Eckman, Patrick H. McCarthy, Scott R. Smedley, Jerrold Meinwald, and Frank C. Schroeder**

Boyce Thompson Institute and Department of Chemistry and Chemical Biology, Cornell University, Ithaca, NY 14853

Department of Biology, Trinity College, Hartford, CT 06106

SUPPORTING INFORMATION TABLE OF CONTENTS

Supporting Methods

1. 2D NMR-spectroscopic screening of insect metabolite samples

1.1. Sensitivity considerations.(1) NMR-spectroscopic analysis of complex mixtures may permit extraction of structural information for very minor components, depending on (1) the amount of sample available and (2) the sensitivity of the spectrometer. Both factors affect the dynamic range of the resulting NMR-spectroscopic data set. From our practical experience with running dqfCOSY spectra on two 600 MHz VARIAN INOVA spectrometers at Cornell University and the 900 MHz VARIAN "Fleckvieh" spectrometer at NMRFAM in Madison, Wisconsin (http://www.nmrfam.wisc.edu/) 0.2 µmol - 1 µmol of a minor component (e.g. 0.1 mg to 0.5 mg of a compound of molecular weight 500) is reliably detected in small molecule mixtures of 10 mg to 50 mg total mass, as long as most of signals of this minor component are not obstructed by other signals. In most cases, useful structural information can be obtained for as little as 0.02 µmol of a trace component in 10 mg of total sample; however, spectral artifacts accompanying signals from major components may prevent analysis when spectral quality is low. In case of the *Delphastus* samples, most of which were in the 10-20 mg range (e.g. example shown in Figure 3), partial structures could be elucidated for compounds representing as little as 0.2% of the total mass of the samples.

1.2. General procedure for 2D NMR-spectroscopic screening.

STEP 1 – SAMPLE PREPARATION. Prepare a sample free from macromolecular compounds (proteins) by filtration over a suitable size-exclusion filter. Considering the polarity of the sample, chose a solvent that dissolves most of the material, remove insoluble component by centrifugation and use the supernatant for spectroscopic analysis. We found that diluting NMR samples with 10% (v/v) of additional NMR solvent following centrifugation greatly reduces the likelihood that of undesirable solid precipitation during acquisition of the spectra. Insoluble components can be analyzed separately using solvent of higher or lower polarity, as needed.

STEP 2 - ACQUISITION OF SPECTRA.(2) Freshly made NMR samples of complex mixtures should be equilibrated for at least 2 h at the temperature that will be used for acquisition of NMR spectra. Subsequently, phase-cycled dqfCOSY spectra (dqfCOSY spectra using gradient-based coherence selection produce inferior results and should NOT be used) are acquired using the following parameters: acquisition time 0.8 s; relaxation delay: 1 s; number of increments: 100 per 1000 Hz of sweep width; number of scans: at least 8, using 16 scans often results in cleaner spectra.

STEP 3 – PROCESSING OF SPECTRA.(2) Spectra are processed using TOPSPIN, VNMRJ, or MNOVA (www.mestrec.com) using the following parameters: number of points in F2: 8192 (small sweep width, 600 MHz) or 16384 (large sweep width, 900 MHz); number of points in F1: 4096; window function in F2: cosine; window function in F1: cosine.

STEP 4 – INTERPRETATION.(2) Interpretation focuses on extracting proton spin systems, i.e. networks of protons represented by signals at specific chemical shift values that are connected by crosspeaks resulting from *J*-coupling. All crosspeaks belonging to a specific spin system are annotated with chemical shift values and coupling constants. Strongest signals representing spin systems of the most abundant compounds are characterized first. In the case of insect-derived samples these are usually fatty acids and fatty acid derived lipids, farnesol, squalene, cholesterol, and related compounds whose proton chemical shifts and spin-spin coupling constants can be easily recognized. Additional analyses by HPLC-MS and GC-MS can assist in identifying common metabolites.

STEP 5 – DEREPLICATION: Spin systems that cannot be attributed to common metabolites are interpreted in terms of *partial structures*, representing structural motifs derived from the signals of one or more crosspeaks. Crosspeaks resulting from long-range proton-proton coupling (for example of methyl groups that appear as singlets in 1D ^{1}H NMR spectra, or allylic couplings of double bond protons, or W-type couplings in rigid ring systems) are of great value at this stage, because they may allow connecting protons separated by more than 3 bonds and thus construction of larger partial structures. If necessary, additional HSQC and HMBC spectra are acquired to clarify additional aspects of the partial structures.

Often several alternative partial structures must be considered, and great care must be taken to keep the proposed partial structures as general as is compatible with the spectral data. These partial structures are then searched against Beilstein, Reaxys, and Scifinder databases. Published NMR spectroscopic data for possible hits are compared with the experimental data and partial structures are confirmed, modified, or discarded based on this comparison. Additional data from HPLC-MS or GC-MS analyses are used to verify any additionally identified known compound and to validate structural assumptions such as incorporation of heteroatoms) in completed new structures.

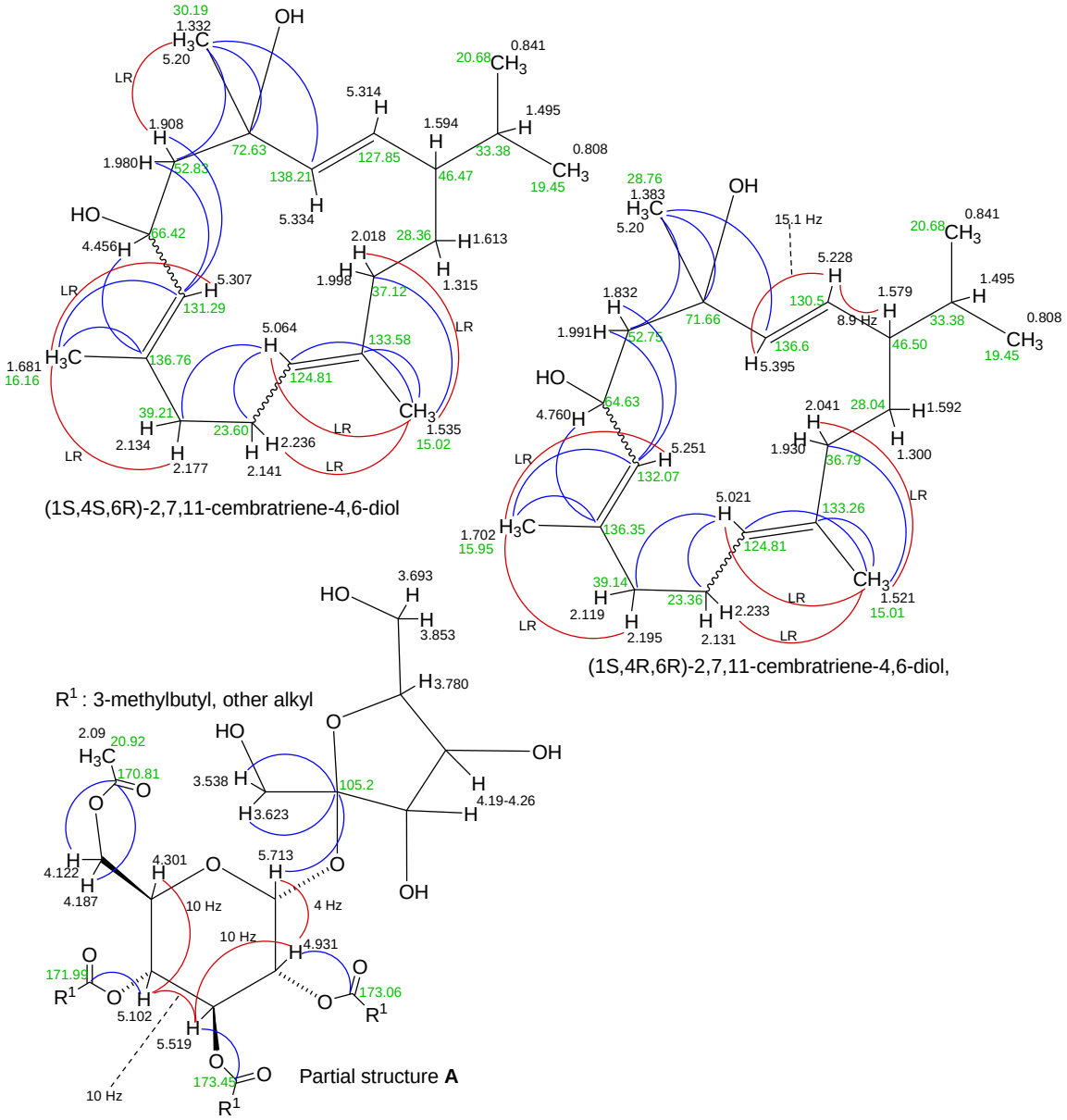

Figure S1. Significant partial structures derived from NMR-spectroscopic analysis of *Heliothis virescens* larval extracts (dqfCOSY, HMQC, and HMBC, CD_2Cl_2, 600 MHz), including chemical shift data as well as significant HMBC correlations (blue) and important coupling constants determined from dqfCOSY spectra (red). LR: long-range (^{1}H,^{1}H)-coupling (J < 2 Hz). For crosspeaks examples representing long-range couplings, see Figure S6.

NMR-spectroscopic data of the two fully characterized cembratrienediols are in agreement with published data,(3) and data for the partially characterized sucrose derivative **A** are consistent with data reported for 6-O-acetyl-2,3,4-tri-O-(3*S*-methylpentanoyl)-α-D-glucopyranosyl-β-D-fructofuranoside, a carbohydrate previously isolated from tobacco.(4) The analysis of the dqfCOSY spectra indicated the presence of at least 5 additional compounds closely related to the cembratrienediols, as well as at least 6 additional compounds with structures related to sucrose derivative **A**. In addition to the shown partial structures, the dqfCOSY spectra showed signals suggesting the presence of saturated and unsaturated fatty acids as well as glycerides.

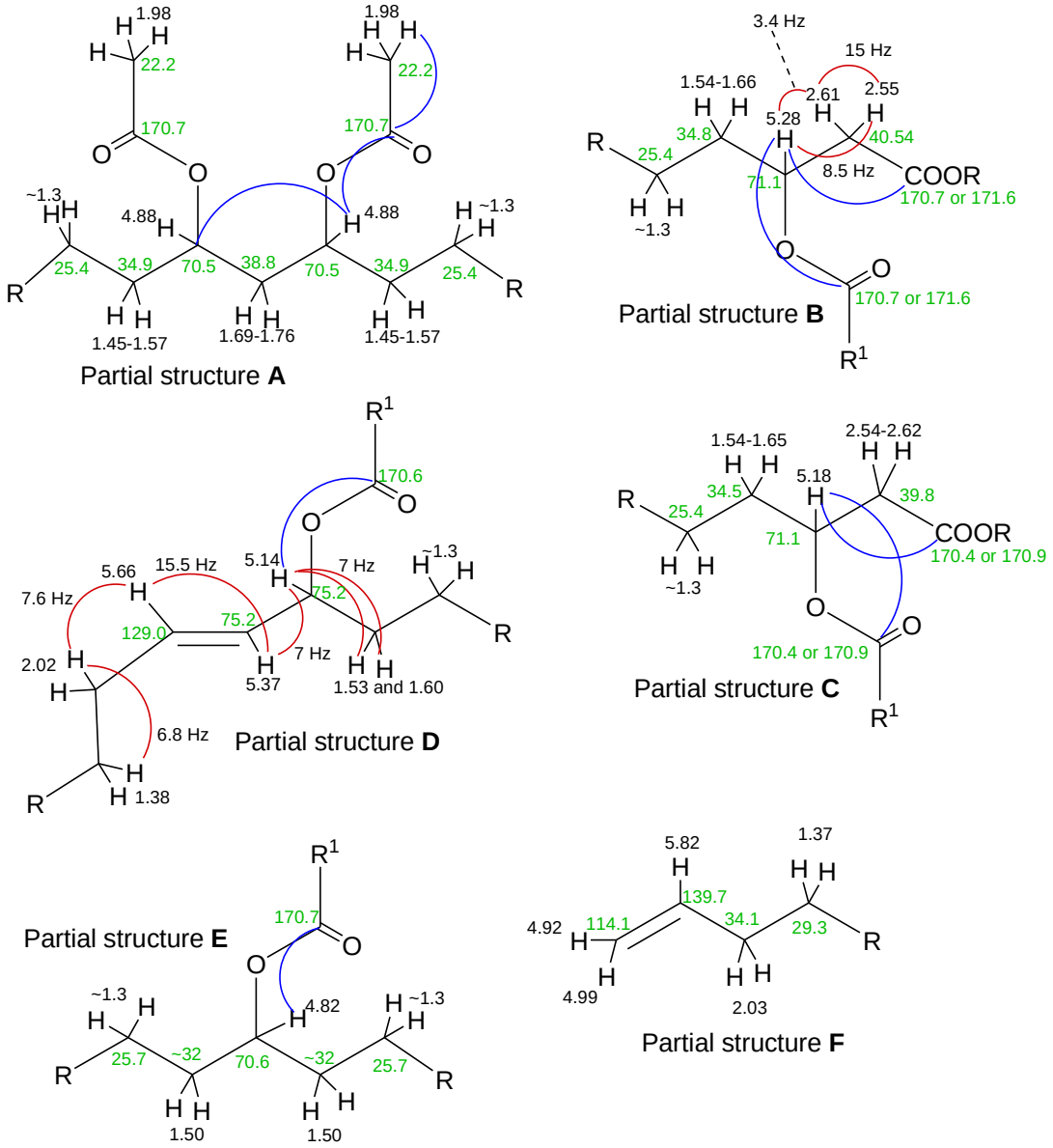

Figure S2. Significant partial structures derived from NMR-spectroscopic analysis of *Schizura unicornis* larval extracts (dqfCOSY, HMQC, and HMBC, CD_2Cl_2, 600 MHz), including chemical shift data as well as significant HMBC correlations (blue) and important coupling constants determined from dqfCOSY spectra (red). LR: long-range (^{1}H,^{1}H)-coupling (J < 2 Hz). For crosspeaks examples representing long-range couplings, see Figure S6.
Partial structure **A** was most abundant. Substituents R and R^1 may represent alkyl, alkenyl, or any of the shown partial structures; R^1 may represent methyl in the majority of cases, as the HMBC provides evidence for the presence of a number of different acetyl groups. In addition to the shown partial structures, spin systems suggesting the presence of mono-, di-, and triglycerides were found. Similar or identical partial structures were detected in *Schizura leptinoides*, *Schizura ipomoea*, and *Agraulis vanilla* samples.

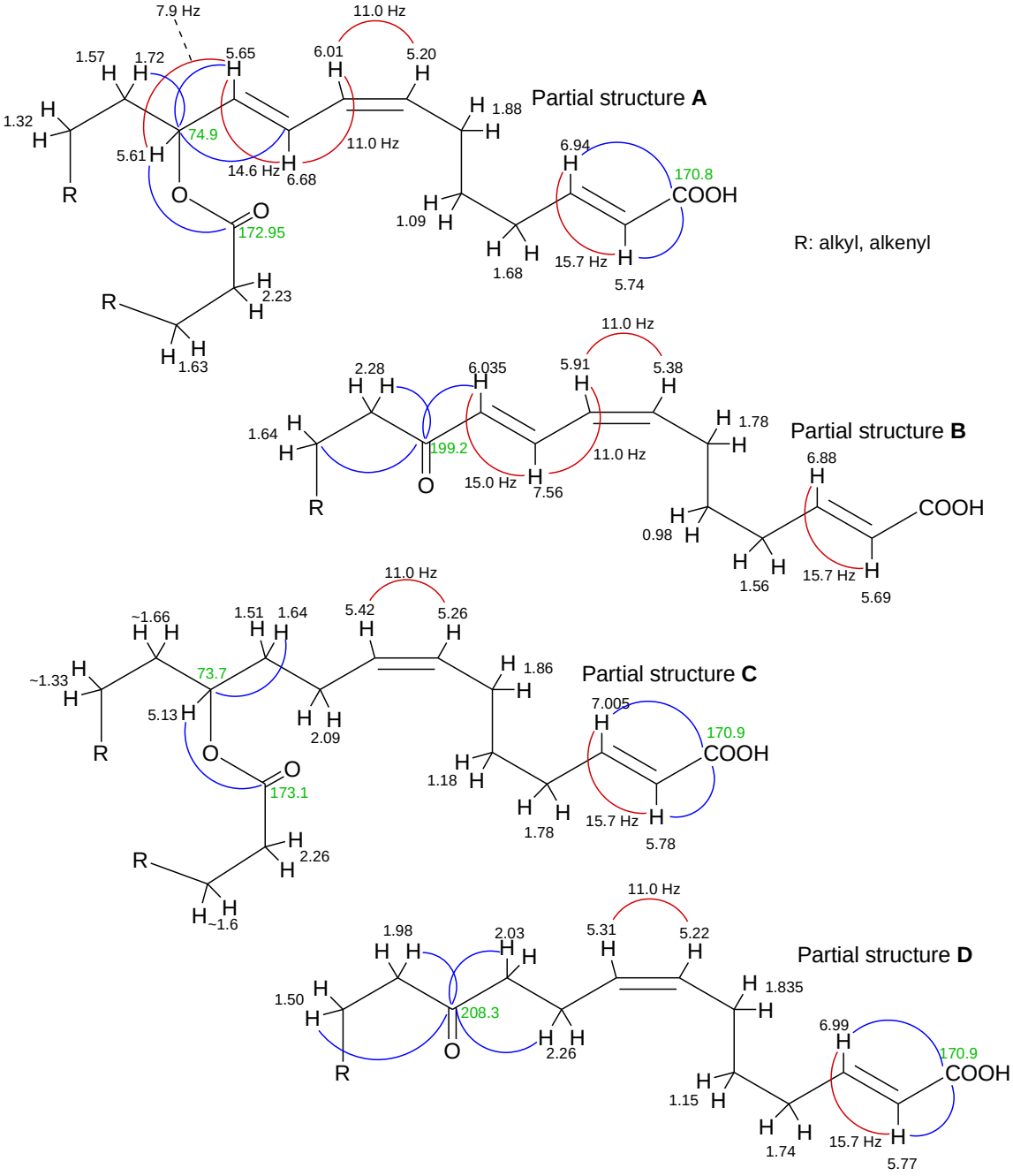

Figure S3. Significant partial structures derived from NMR-spectroscopic analysis of *Pieris napi* and *Pieris virginensis* larval extracts (dqfCOSY, HMQC, and HMBC, C_6D_6, 600 MHz, R^2: alkyl, alkenyl, or any of the shown partial structures), including chemical shift data as well as significant HMBC correlations (blue) and important coupling constants determined from dqfCOSY spectra (red). All four partial structures were present in *P. napi* extracts, whereas *P. virginensis* extracts contained only partial structures **C** and **D**.

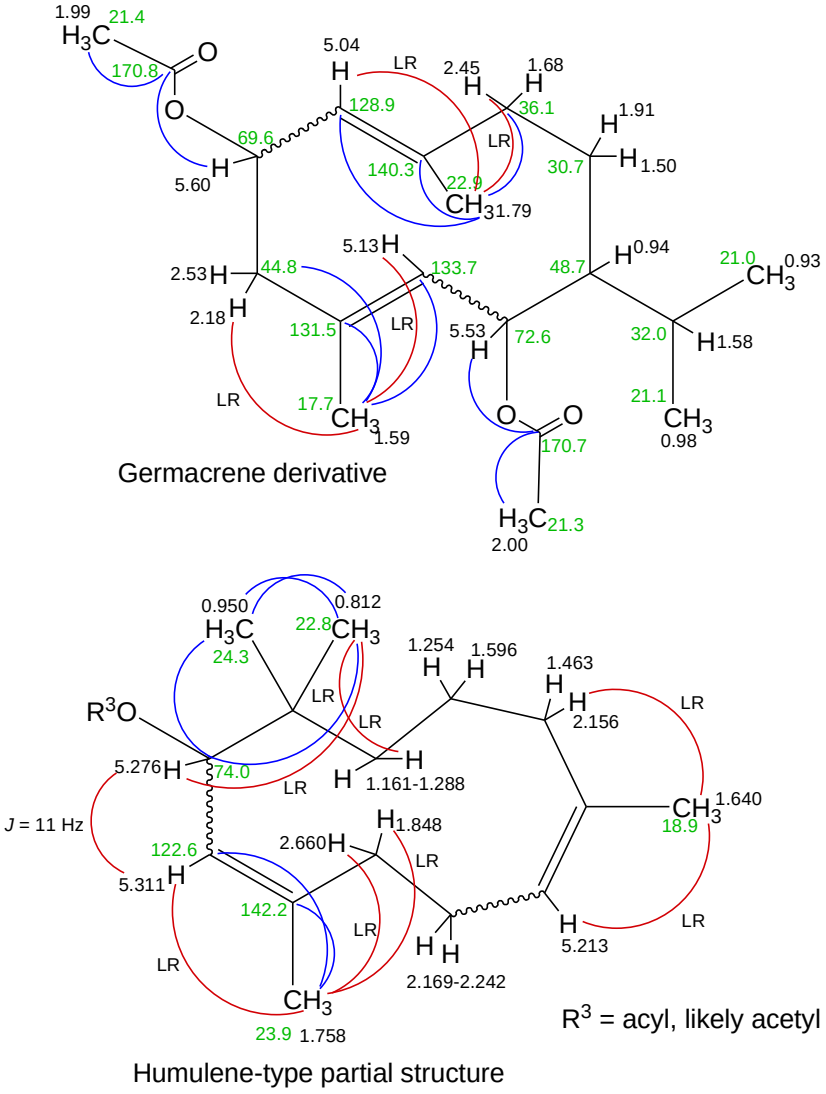

Figure S4A. Significant partial structures derived from NMR-spectroscopic analysis of *Delphastus catalinae* pupal extracts (dqfCOSY, HMQC, and HMBC, CD_2Cl_2, 600 MHz), including chemical shift data as well as significant HMBC correlations (blue) and important coupling constants determined from dqfCOSY spectra (red). LR: long-range ($^1H,^1H$)-coupling (J < 2 Hz). For crosspeaks examples representing long-range couplings, see Figure S6.

Several additional terpenoids with similar structures were also detected, in addition to large amounts of farnesol, triglycerides, and fatty acids. For partial structures representing the catalipyrones, **see next page for Figure S4B**.

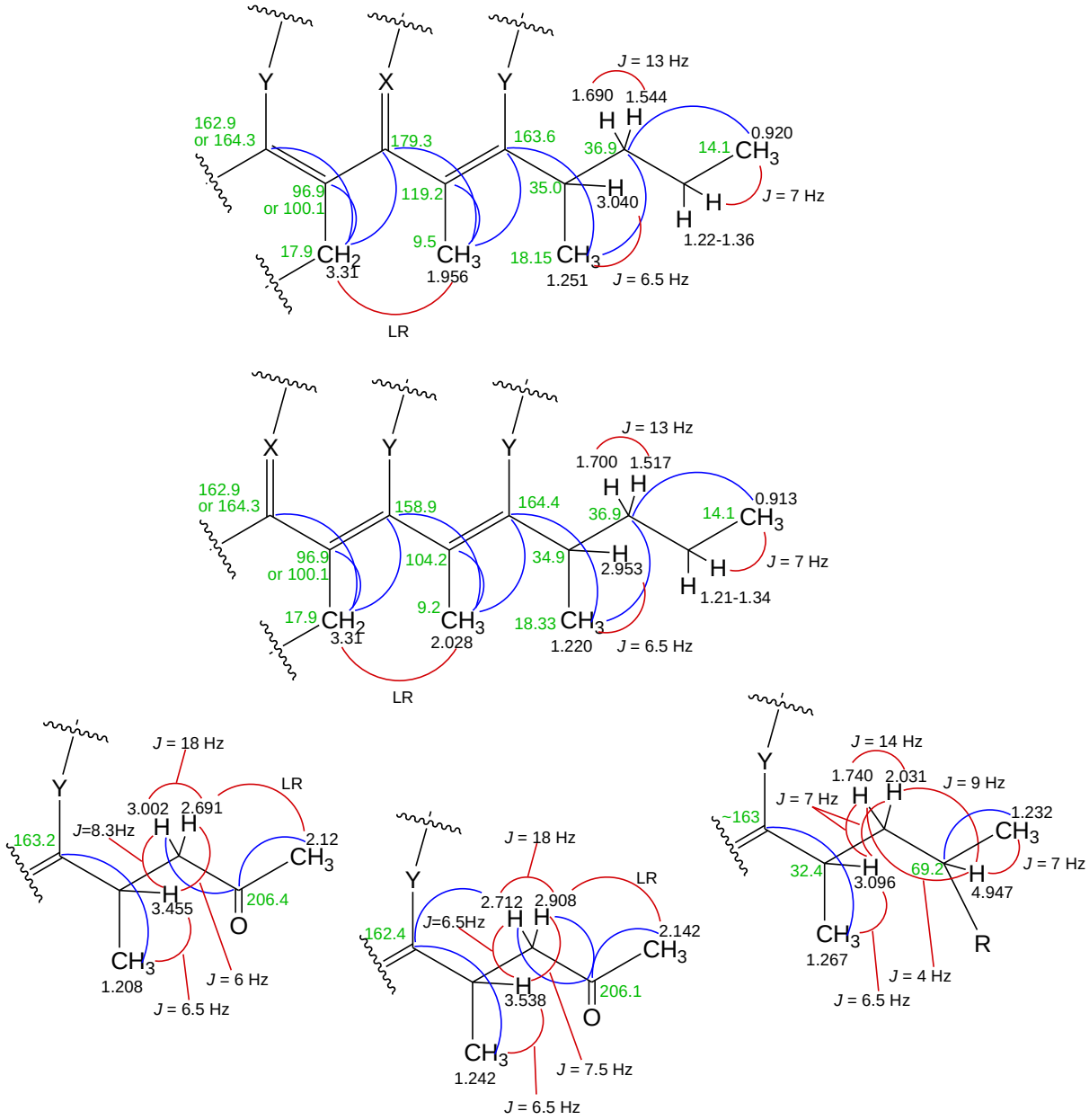

Figure S4B. Polyketide-like partial structures derived from NMR-spectroscopic analysis of *Delphastus catalinae* pupal extracts (dqfCOSY, HMQC, and HMBC, CD_2Cl_2, 600 MHz), including chemical shift data as well as significant HMBC correlations (blue) and important coupling constants determined from dqfCOSY spectra (red). Shown here are partial structures representing the most abundant polyketides in the extract. Smaller amounts of several related compounds were detected as well. LR: long-range (^{1}H,^{1}H)-coupling (J < 2 Hz). For crosspeaks examples representing long-range couplings, see Figure S6. Solely considering the results of NMR-spectroscopic analysis of the unfractionated extracts, the shown chemical shifts suggested X = O, N and Y= C, N, O, or S, as well as R = acyloxy, possible acetate.

Analysis of whole-body extracts of adult *Delphastus* revealed several additional variants, some of which are shown in Figure 2, for example, partial structures featuring a hydroxy in place of the keto group shown here. **Full NMR spectroscopic data for all 10 isolated pupal and adult polyketides, including all proton and carbon signals, coupling constants, and HMBC correlations, are listed in Tables S3-S12.**

Table S1. Abbreviated list of partial structures detected in NMR-spectroscopic structure gazing of the 10 insect species in this study.

Species	Stage 1: dqfCOSY	Stage 2: HSQC/HMBC
Delphastus catalinae pupae and adults	**Spin systems suggestive of terpenoids and/or polyketides, glycerides, fatty acids**	- Farnesol, germacrene, and humulene derivatives **- Polyketides**
Pieris napi	**Functionalized fatty acids**	Acyloxy-substituted fatty acids, similar to known compounds
Pieris virginensis	**Functionalized fatty acids**	Acyloxy-substituted fatty acids, similar to known compounds
Anthocharis midea	Fatty acids, glycerides	*(Not pursued)*
Agraulis vanillae	Trace amounts of functionalized fatty acids	*(Not pursued)*
Megisto cymela	Fatty acids, glycerides	*(Not pursued)*
Schizura ipomoeae	Fatty acids, glycerides	*(Not pursued)*
Schizura unicornis	**Functionalized fatty acids, glycerides, fatty acids**	Acyloxy-substituted fatty acids, similar to known compounds
Schizura leptinoides	Fatty acids, glycerides	*(Not pursued)*
Heliothis virescens	**Terpenoids, carbohydrate derivatives, fatty acids**	Known cembratrienediol-type diterpenoids; known poly-acyl sucrose derivative plus several related compounds

2. Structure determination.

2.1. Structure elucidation of 2,6,10-trioxa-1,11-dioxoanthracenes.

Catalipyrone A (1). The carbon-carbon connectivity of the side-chain of **1** (C-1′–C-4′ and 1′-CH_3) was easily assigned via analysis of 1D and 2D NMR spectra, including dqfCOSY data (Figures S2-S5). Both ^{13}C NMR and ^{1}H NMR chemical shift data for C-3′ indicated the presence of an oxygen at that position. The ^{1}H NMR spectrum revealed a broad doublet that coupled to oxymethine H-3′ when observed in acetone-d_6 that was absent in spectra acquired in methanol-d_4, thus allowing the assignment of the oxygen at C-3′ to be an alcohol. Methyl group 1′-CH_3 showed a correlation to C-3, an oxygenated olefin (δ_C 164.5) in the HMBC spectrum. Aryl methyl 4-CH_3 had correlations to C-3, C-4, and C-5, in the HMBC, thus allowing for the partial structure to be extended from C-5 through C-4′. HMBC correlations from H_2-13 to C-1, C-5, and C-14 provided evidence for an uninterrupted carbon chain from C-1–C-4′ with three branches, two methyl groups (4-CH_3 and 1′-CH_3) and a methylene unit (C-13).

The HSQC correlation for H_2-13 indicated that it was a methylene unit, however this signal integrated as a single proton in the ^{1}H NMR spectrum, thus indicating that **1** was symmetrical around C-13. This along with the ESI-MS data (Figure S1), which indicated a molecular mass of 418 based on an M+H of 419 and M+Na of 441, allowed for determination of the molecular formula ($C_{23}H_{30}O_7$, 9 units of unsaturation). Carbons C-3/9 and C-5/7 were determined to be oxygenated olefins based on their chemical shift values (δ_C 160.4 and 164.5, respectively) and the fact that they were each bonded to two additional carbons, thus ruling out the possibility of them being ester moieties. Carbons C-1/11 had chemical shift values indicating that they were either oxyolefins or oxycarbonyls (δ_C 165.0), but since all 21 other carbons had already been assigned, they could not be oxyolefins, thus allowing for their assignment as either esters or carboxylic acids. The latter possibility was ruled out based on the molecular formula.

Six units of unsaturation are accounted for by the presence of two esters and four olefins, thus indicating that there must be three rings in the molecule. Since carbon-carbon connectivity was already established, the rings must all be connected through oxygens. The oxygens on methine carbons C-3′/3″ could not be incorporated in rings since they were determined to be alcohols. There remained two possibilities, 1) two six-membered pyrones and a six-membered pyran, or 2) two four-membered pyrones and a ten-membered ether-linked ring. The former ring-system was chosen due to

relative stabilities and comparison of carbon chemical shifts to literature values,(5) thus completing the assignment of the planar structure of **1**.

2.2. Determination of the absolute configuration of compound 1. The absolute configuration of C-3′/3″ was determined through analysis of ^{1}H NMR data of the (*R*)- and (*S*)-MTPA-ester derivatives of **1** (Figure S6), which were prepared as follows. To two samples of compound **1** (each 0.20 mg, 0.48 μmol) solutions of DMAP in dichloromethane-d_2 (200 μl, 1.3 μg/μL) and (*R*)- or (*S*)-Mosher chloride (200 μL, 33μg/μL) in dichlorometane-d_2 were added. The resulting mixtures were stirred at 23 ºC for 4 h in the dark. The resulting samples of (*S*)- and (*R*)-MTPA derivatives (note that treatment of **1** with (*R*)-Mosher chloride yielded the (*S*)-MTPA ester) of compound **1** were analyzed directly by ^{1}H NMR spectroscopy (600 MHz) using Shigemi tubes.

Proton signals from 1′-C<u>H</u>$_3$/1″-C<u>H</u>$_3$, H-1′/H-1″, and H$_2$-2′/H$_2$-2″ all showed a positive $\Delta\delta^{SR}$ whereas H$_3$-4′/H$_3$-4″ showed negative $\Delta\delta^{SR}$, indicating that C-3′ and C-3″ had an *S* configuration. The molecular model for both possible relative configurations (3′/3″ *S*, 1′/1″ *R* and 3′/3″ *S*, 1′/1″ *S*) were constructed using ChemBio3D Ultra (Cambridgesoft) and energies were minimized using an MM2 algorithm (Figure S7). The *S/S* model predicted a positive cotton effect upon analysis by circular dichroism, while the *S/R* model showed significant mass in both the positive and negative quadrants. The observed CD spectrum displayed a negative cotton effect supporting assignment of C-1′ and C-1″ as *R* (Figure S8). In addition, the *S/R* model predicted a dihedral angle of 62° between H-1′ and H-2′a, and 177° between H-1′ and H-2′b, whereas the *S/S* model predicted 87° and 25° angles, respectively, between these protons. The dihedral angles of the *S/R* model more closely match what one would expect based on the coupling constants observed between H-1′ and H-2′a (J_{HH} = 4.1 Hz) and those between H-1′ and H-2′b (J_{HH} = 11 Hz). Therefore the configuration at position 6/6′ is proposed to be *R*. This assignment is further supported by the similarity of the ^{1}H NMR chemical shift data to those of similar *R/S* sidechains on aromatic rings described previously.(6, 7)

2.3. Structure elucidation of 4,8-dioxo-1,9,13-trioxaanthracenes.

Catalipyrone H (8). The molecular weight of compound **8** was determined to be 386 from LC-MS data (+ESI-MS showed peaks at *m/z* 387 and 773, $[M+H]^+$ and $[2M+H]^+$, respectively). This mass being 32 amu less than **1**, in conjunction with the absence of any oxymethine signals in the ^{1}H NMR

indicated a likely molecular formula of $C_{23}H_{30}O_5$, which was subsequently confirmed via HRMS (Table S10).

The planar structure was then readily assembled from the ^{1}H NMR and HMBC data. HMBC correlations from methyl groups H_3-4′, 1′-C$\underline{H}_3$, H_3-4″, and 1″-C$\underline{H}_3$ to nearby carbons allowed for the two side-chains to be elucidated. Whereas HMBC correlations from methylene unit H_2-6, along with those from methyl groups 11-C$\underline{H}_3$ and 3-C$\underline{H}_3$ allowed for connection of all 23 carbons (Figure S9). This analysis of the HMBC spectrum, along with the molecular formula allowed for assignment of the 4,8-dioxo-1,9,13-trioxaanthracene ring-system. The absolute configurations at position 1′/1″ is proposed to be *R* by analogy to compound **1** since the ^{1}H and ^{13}C NMR data for CH-1′ and 1′-C$\underline{H}_3$ so closely match, and since the biosynthetic machinery is likely to produce only one configuration at this stereocenter.

Catalipyrone J (10). The structure of **10** was primarily assigned based on spectroscopic similarities to compounds **8** and **9**. The mass spectrometric data indicated that **10** was 58 amu heavier than **8**. This, along with the NMR spectroscopic data indicated the presence of an acetate moiety at position 3′ (Table S12). The absolute configuration of position 3′ is proposed to be *R* (as in compound **3**) based on chemical shift values and proton coupling patterns observed in the ^{1}H NMR. This assignment is further supported by the isolation of trace amounts of a compound epimeric to **10** at position 3′. The compound was not present in sufficient quantities to fully characterize, however the ^{1}H NMR revealed it to more closely match the chemical shift and coupling data of **2**, thus reinforcing our configurational assignment of **10**.

3. Ant Bioassay. To possible insect deterrent properties of catalipyrone A (**1**), the isolated compound's effect on the foraging behavior of *C. lineolata* was determined. Within a colony's box, ants were trained to forage from a plastic dish (9 cm diameter) upon which was placed a glass microscopy coverslip (22 x 22 mm; with a central silicone dab serving as a handle) bearing several chopped mealworms at least several hours prior to the start of a trial. Compound **1** was topically applied as a solution in dichloromethane (4.35 µg of **1** in 1 µL) to the surface of vestigial-winged fruit flies (*Drosophila melanogaster*) that had been killed by freezing. The catalipyrone A-coated fruit fly was placed on a corner of a coverslip (experimental), and at the diagonally opposite corner was placed a solvent control *Drosophila* that had received topical application of simply 1 µL of dichloromethane. Treatment and control positions were alternated between trials. In the middle of the coverslip were

placed two mealworm pieces (3-5 mm long) to help ensure ant foraging in the vicinity of the *Drosophila*.

Trials (n = 25) were initiated with the removal of the training coverslip from the dish and its replacement with the experimental coverslip. At 1-min intervals over 1 h, the position (in original location; moved by ant, but on dish; removed from dish) of each *Drosophila* was recorded. At the close of the trial, the fate of each *Drosophila* was recorded as "remaining," if still on the dish, or "removed," if the foraging ants had carried it off the dish. A second series of foraging trials (n = 38) was conducted to compare the activity of compound **1** with several other substances applied separately at 4.35 µg in 1 µl of methylene chloride to *Drosophila*: (±)-nicotine (≥ 98%), hexadecanoic acid (≥ 99%), and (±)-α-tocopherol acetate (≥ 96%). The relative positions on the coverslip of the three treatments and a methylene chloride solvent control were alternated between trials. Foraging ant colonies removed significantly lower numbers of catalipyrone A-coated *Drosophila* than control. Of the 38 methylene chloride control *Drosophila*, only 7 (18.4%) remained after 1 hour, whereas 20 out of 25 (80%) of the catalipyrone A-treated *Drosophila* remained after 1 hour. The most potent of the standard compounds tested was nicotine, a known anti-insectan compound, which had 50% of *Drosophila* remaining after 1 hour.

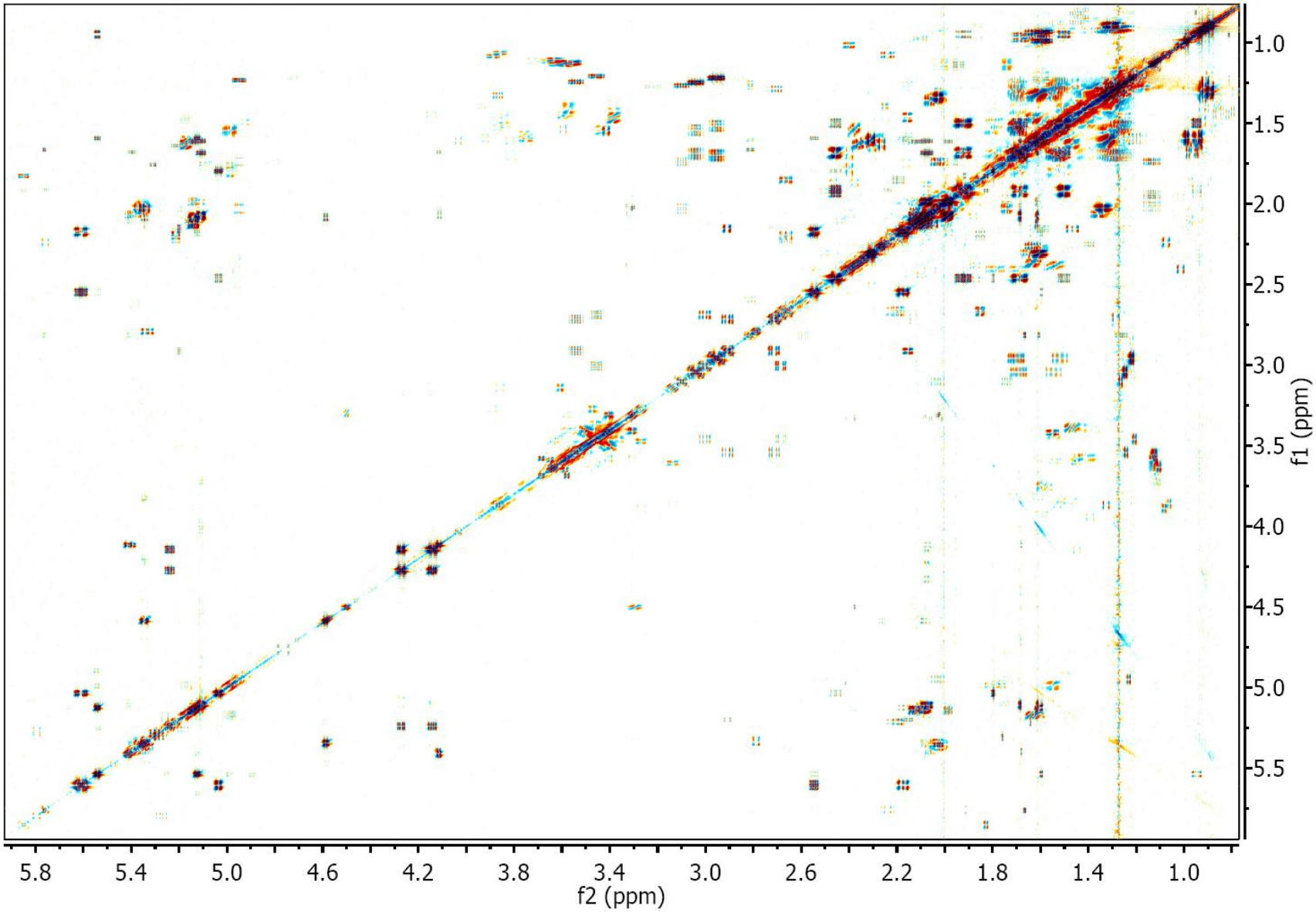

Figure S5. dqfCOSY spectrum of the pupal *D. catalinae* extract (CD_2Cl_2, 600 MHz).

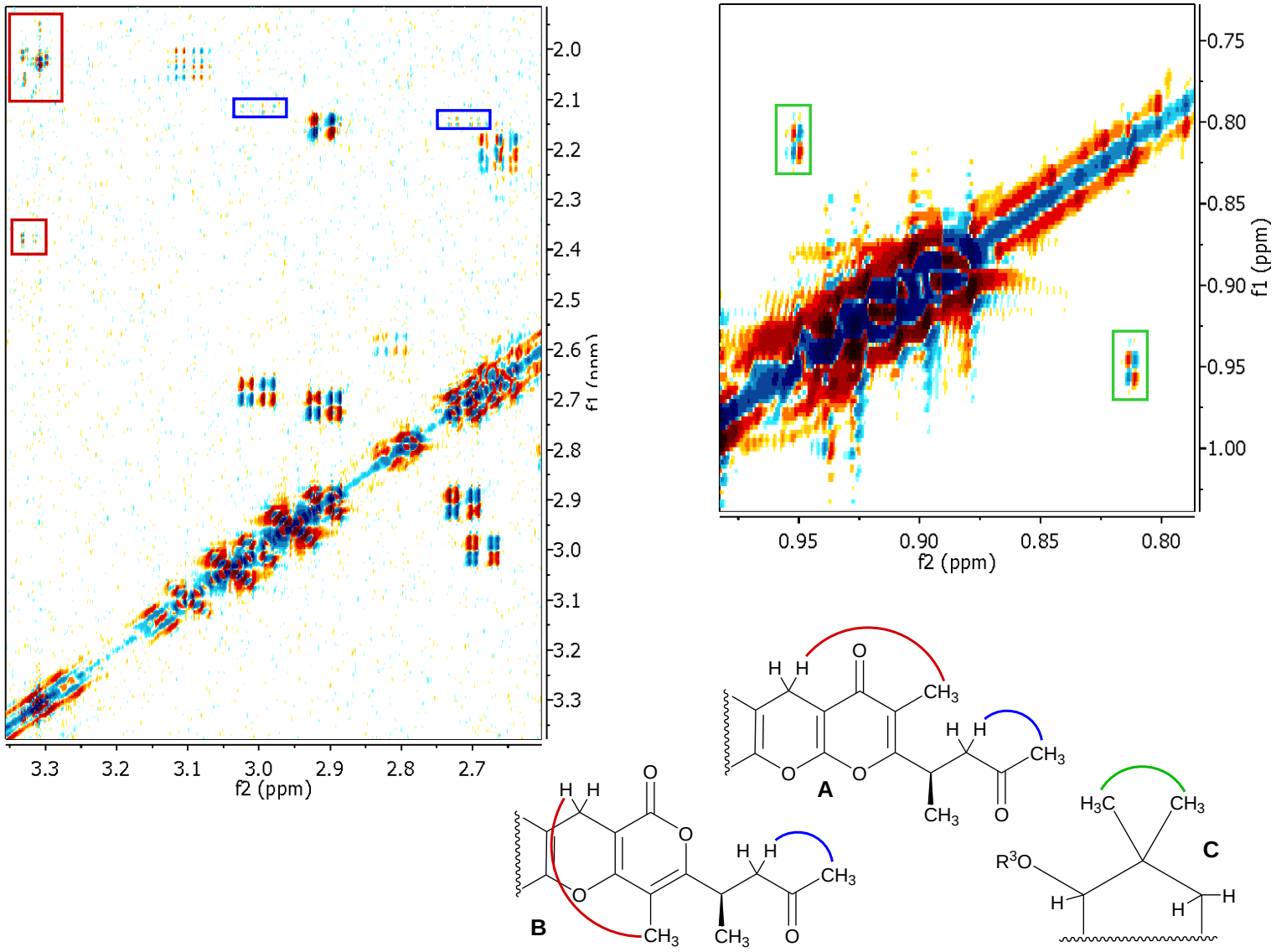

Figure S6. Detail of dqfCOSY spectrum of the pupal *D. catalinae* extract (CD_2Cl_2, 600 MHz), showing (^1H,^1H)-long-range couplings between distant structural features (protons separated by 3 or more bonds) in catalipyrones (red and blue) and a terpenoid (green).

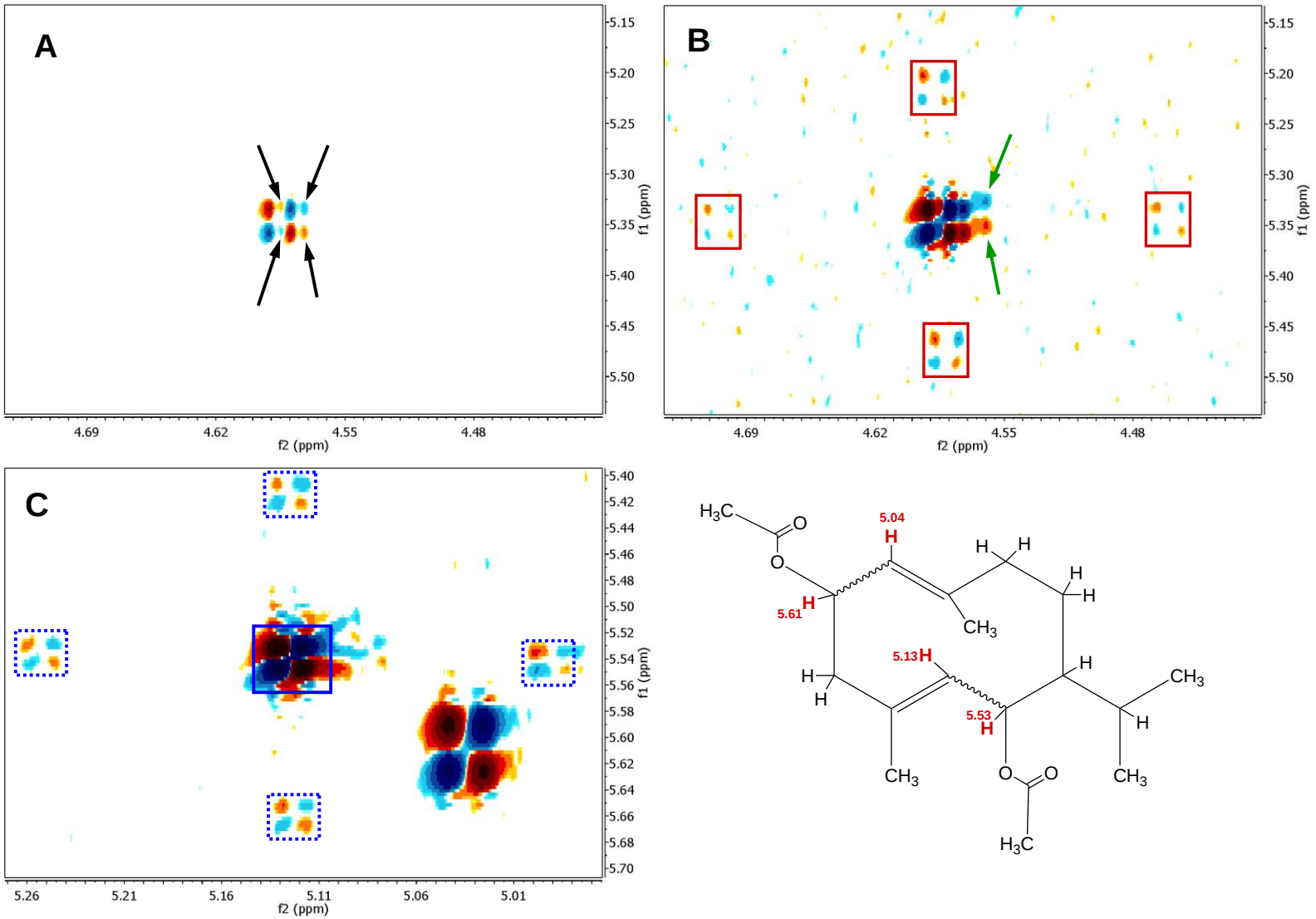

Figure S7. Section of dqfCOSY spectrum of pupal *D. catalinae* extract (CD_2Cl_2, 600 MHz), illustrating the dynamic range of dqfCOSY spectra. **A:** Section showing crosspeak of the CH_2-O group in *trans*-farnesyl acetate. Analysis of the fine structure of this crosspeak reveals presence of a minor component (black arrows), likely a double-bond isomer. **B:** Same section as shown in **A**, with spectral display intensity increased, revealing ^{13}C-satellites (red squares) of the main crosspeak in **A**, as well as additional minor components (green arrows). The intensity of the ^{13}C-satellites is 0.5% of that of the main crosspeak. Farnesyl acetate is one of the major components of the pupal extract, accounting for roughly 10% of its mass; therefore farnesyl acetate containing a $^{13}CH_2$-O group accounts for roughly 0.1% of the total extract. **C**: Section showing two crosspeaks of the major germacrene derivative (representing the protons highlighted in red in the structure). ^{13}C-satellites are well visible for one of the two crosspeaks (for complete assignment of this germacrene derivatives, see Figure S4A).

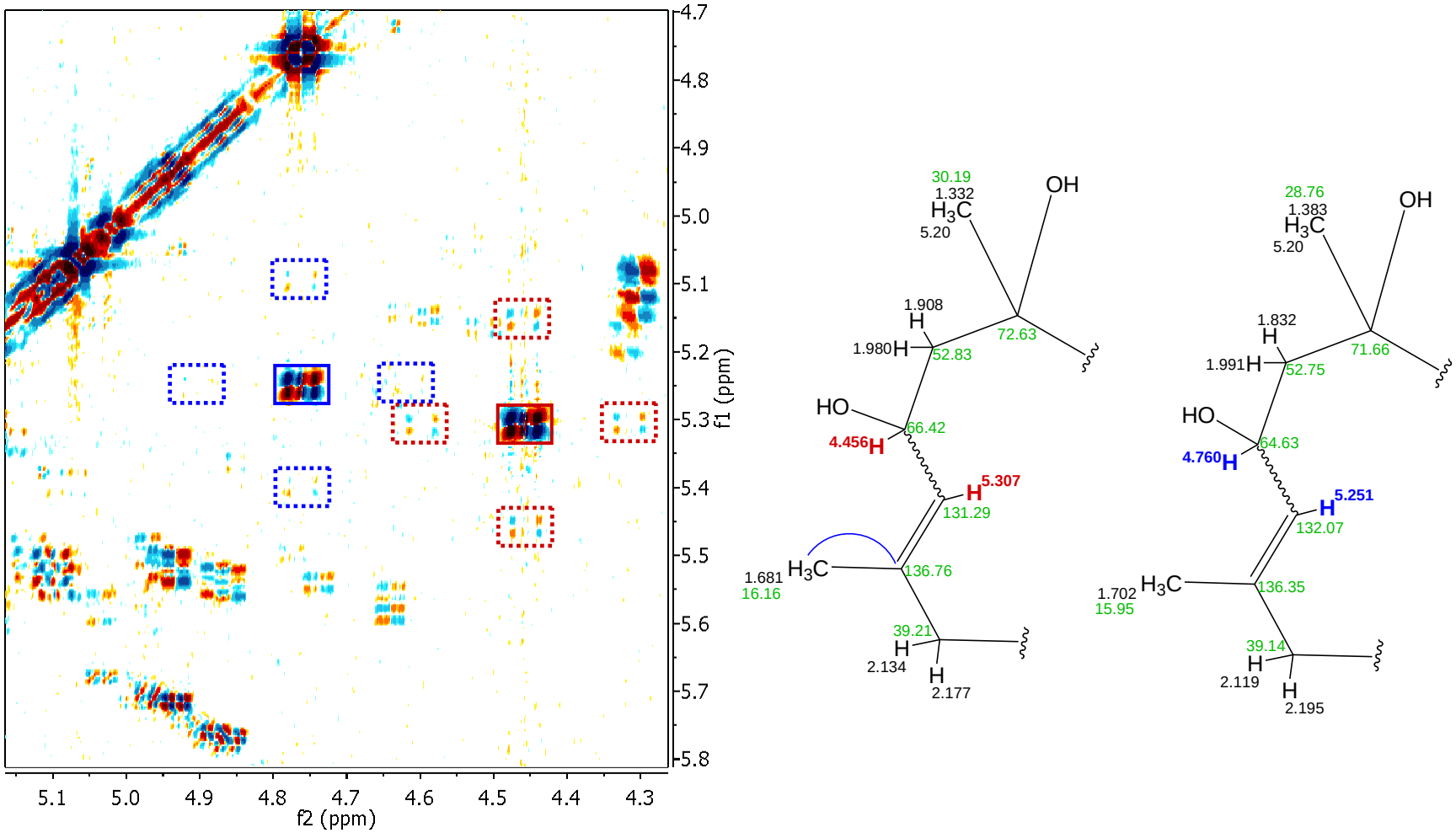

Figure S8. Section of dqfCOSY spectrum of *Heliothis virescens* larval extracts (CD_2Cl_2, 600 MHz), illustrating dynamic range of dqfCOSY spectra. This section shows crosspeaks of double bond protons in the two cembratrienediols (marked red and blue) described in Figure S1. The ^{13}C-satellites (dashed red squares) of the more abundant cembratrienediol (accounting for ~20% of the total extract) are well distinguished, whereas ^{13}C-satellites of the slightly less abundant cembratrienediol (dashed blue squares, about half as abundant) are only slightly above the noise level. For complete assignment of the two cembratrienediols, see Figure S1.

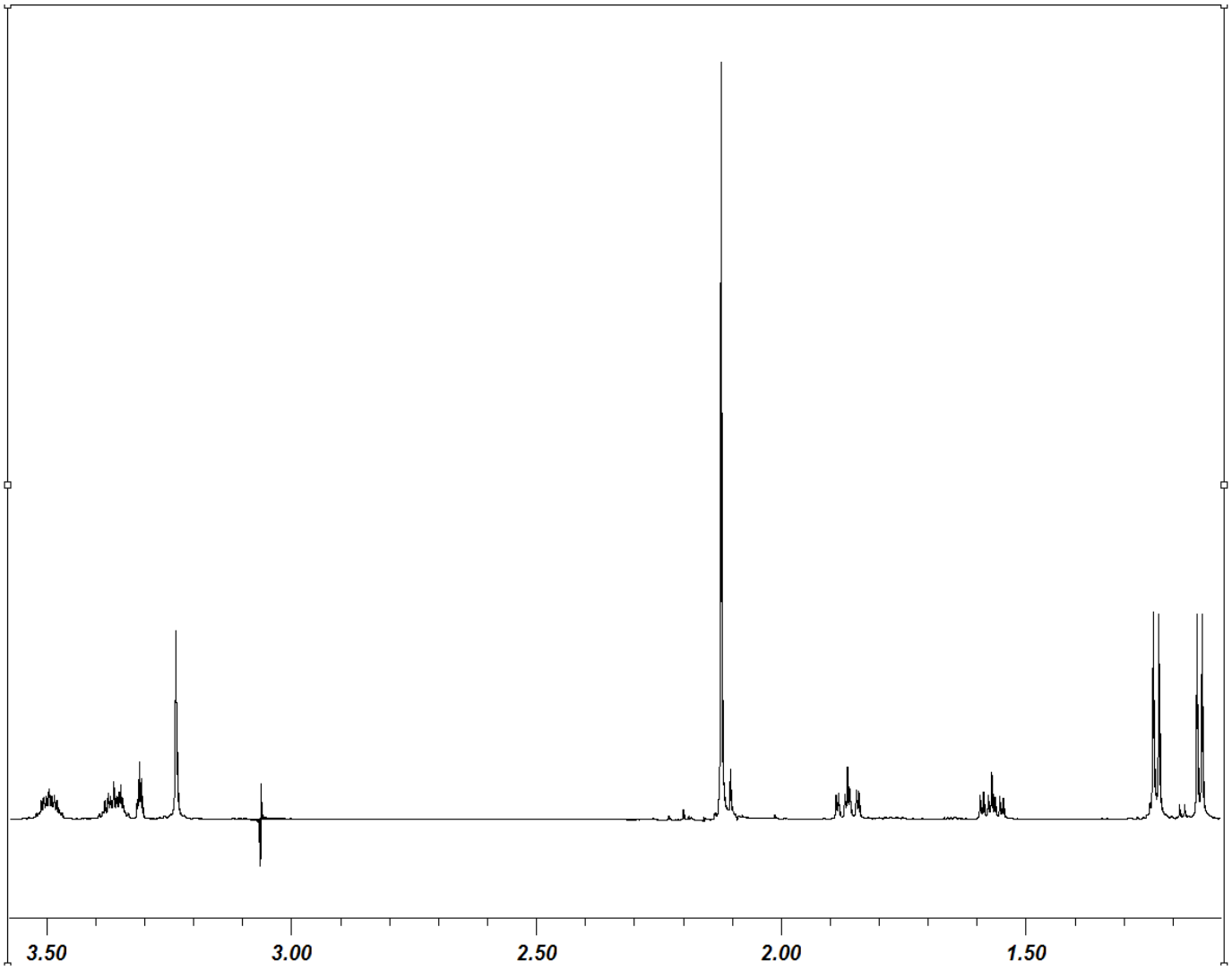

Figure S9. ^{1}H NMR spectrum of pure catalipyrone A (**1**) in CD_3OD at 600 MHz.

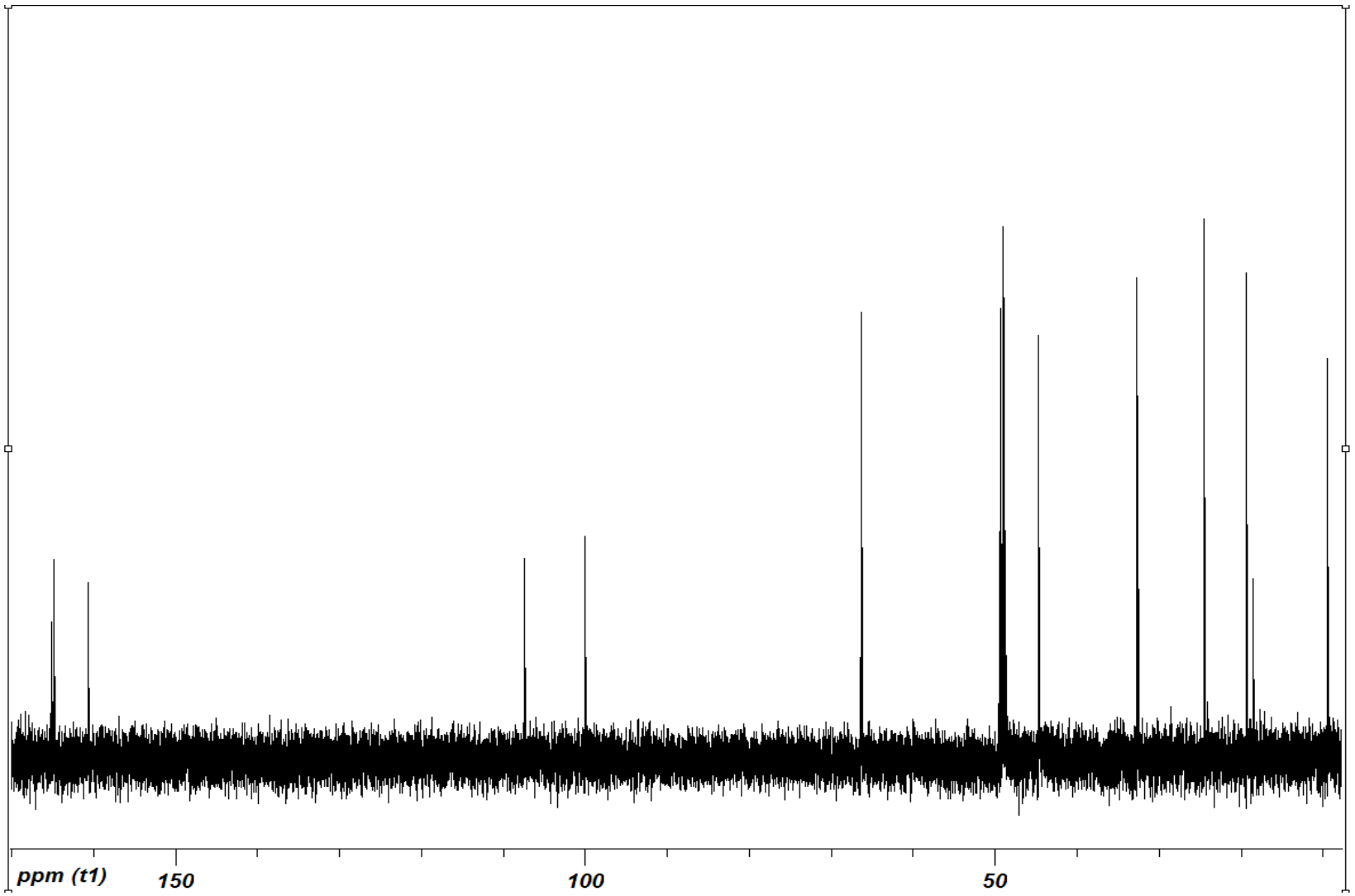

Figure S10. ^{13}C NMR spectrum of **1** in CD_3OD at 125 MHz.

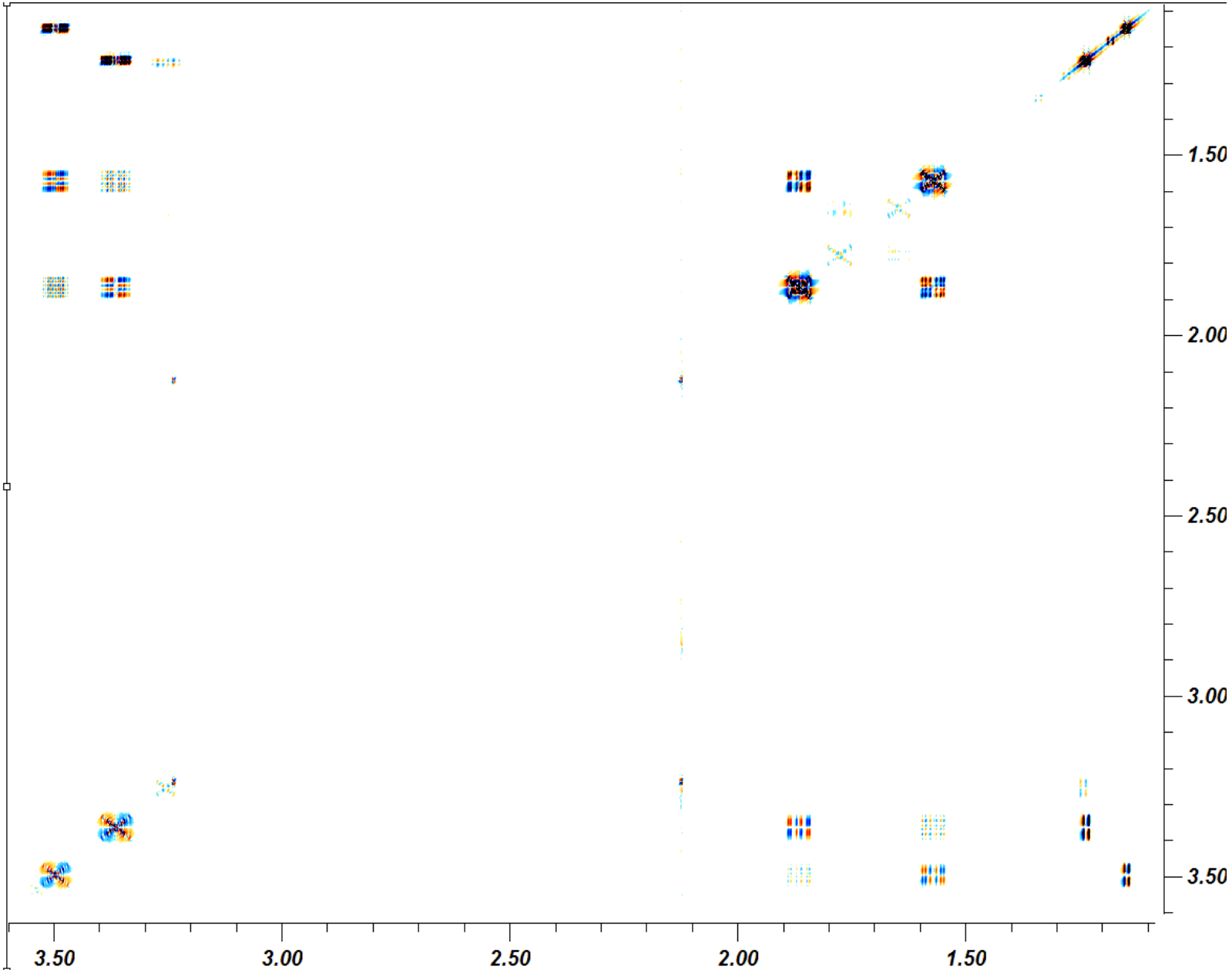

Figure S11. dqfCOSY spectrum of **1** in CD_3OD at 600 MHz. Chemical shifts in ppm.

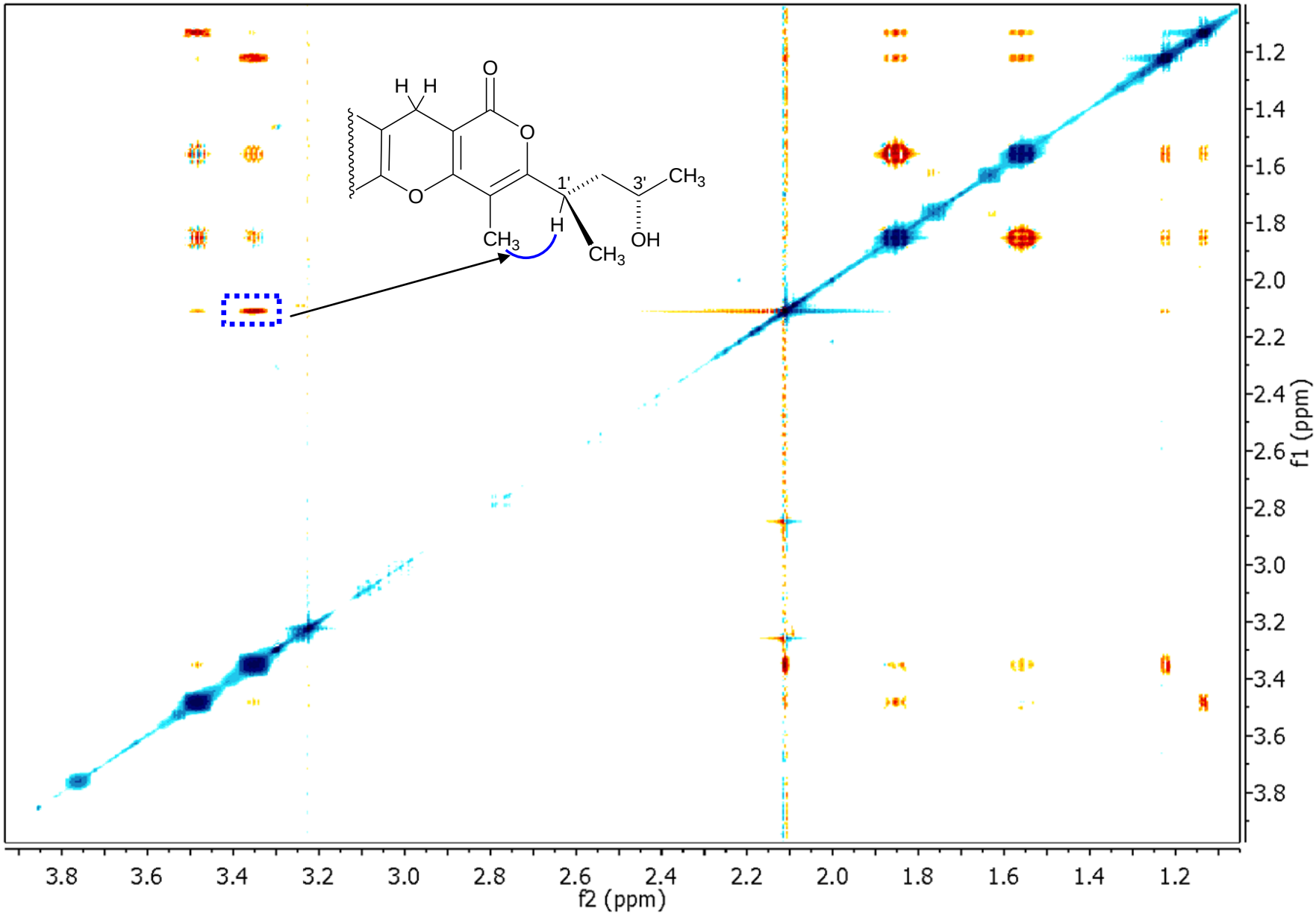

Figure S12. NOESY spectrum of **1** in CD_3OD at 600 MHz. The presence of a strong NOE (marked blue) between the aromatic methyl group and the proton in position 1' of the side chain, in conjunction with the absence of significant NOE's between the aromatic methyl group and other protons of the side chain, defines the side chain's conformation as shown. Also compare Figure S18A.

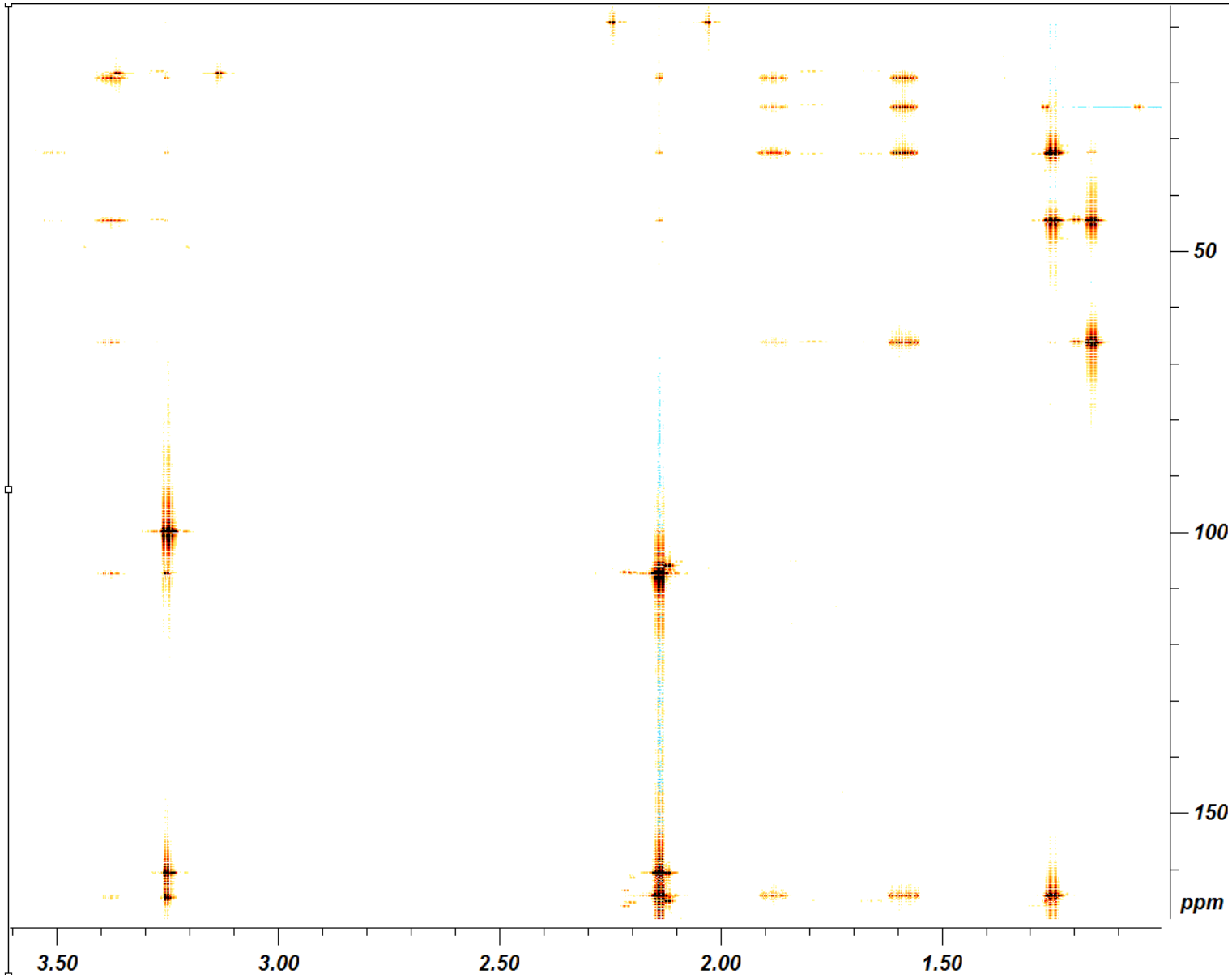

Figure S13. HMBC spectrum of **1** in CD_3OD at 600 MHz (chemical shifts in ppm).

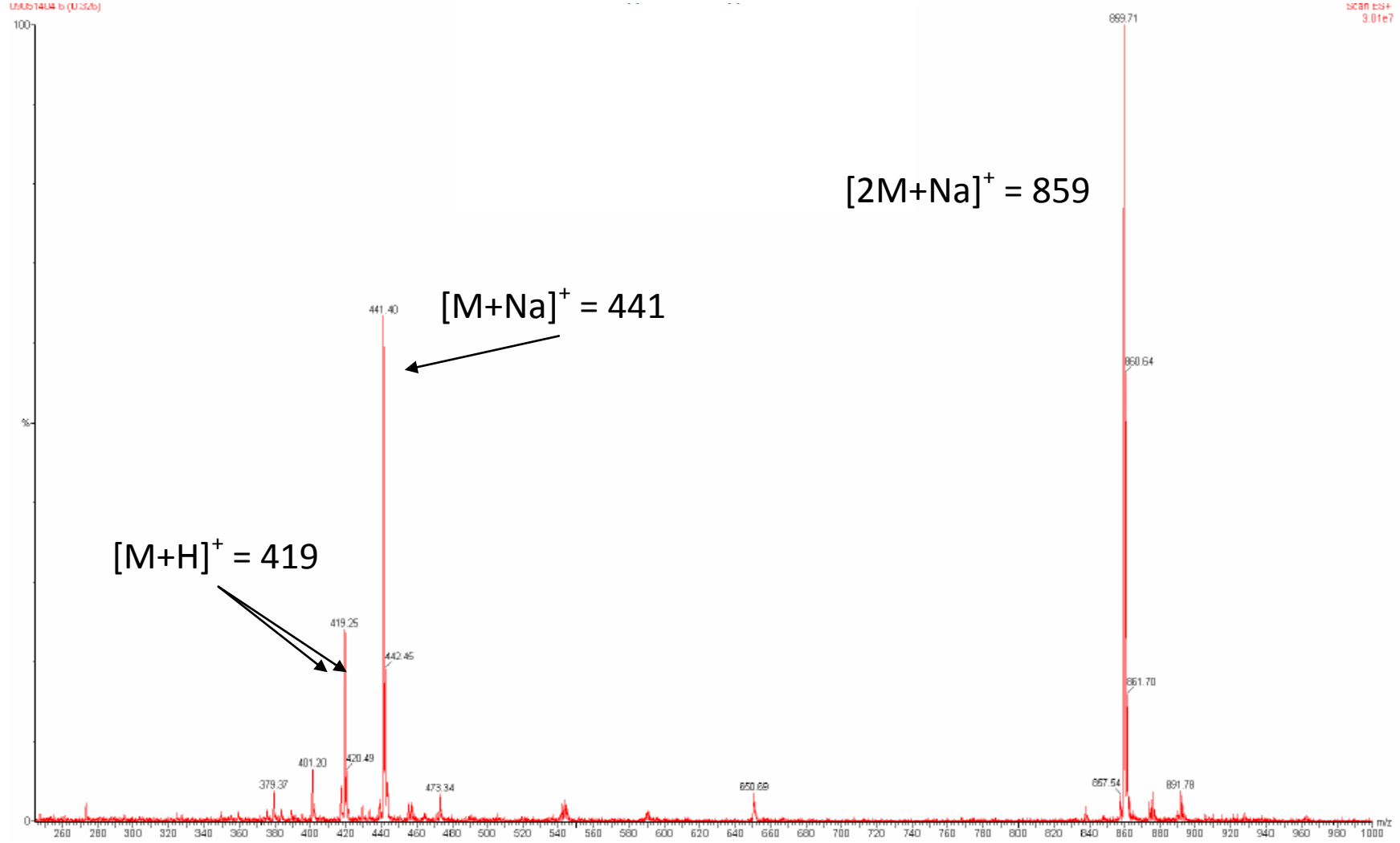

Figure S14. ESI-MS spectrum for compound **1**.

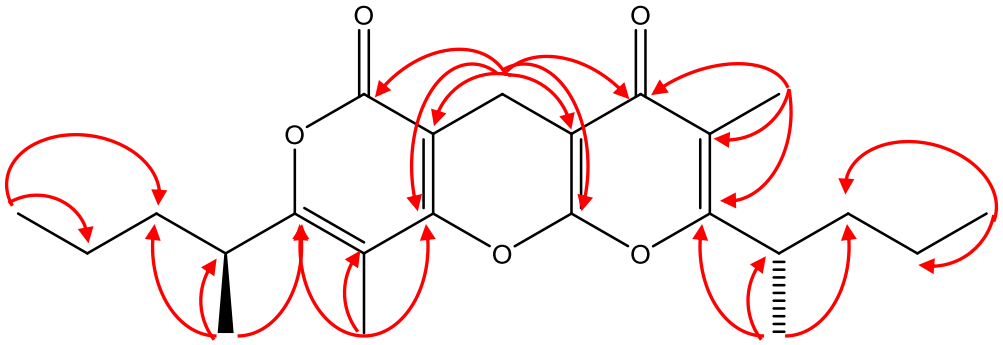

Figure S15. Key HMBC correlations for **8**.

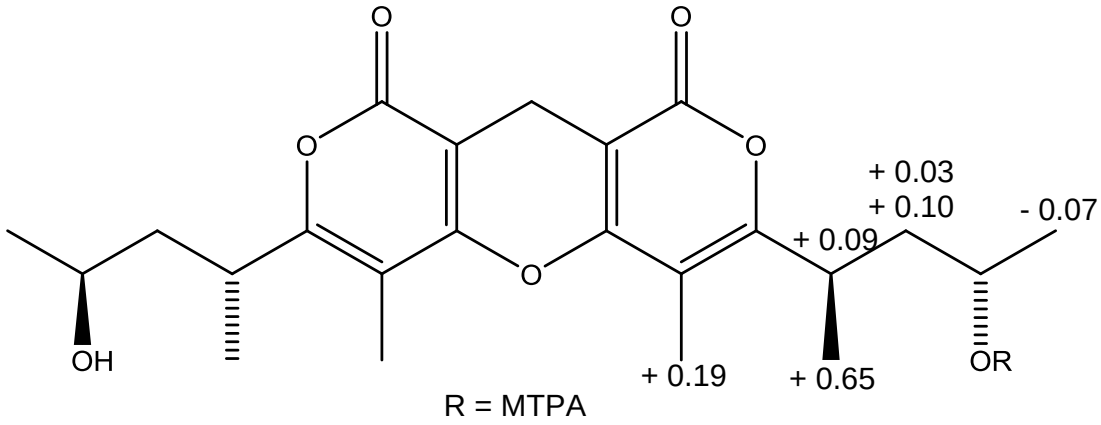

Figure S16. $\Delta\delta^{SR}$ values for the MTPA ester of **1**.

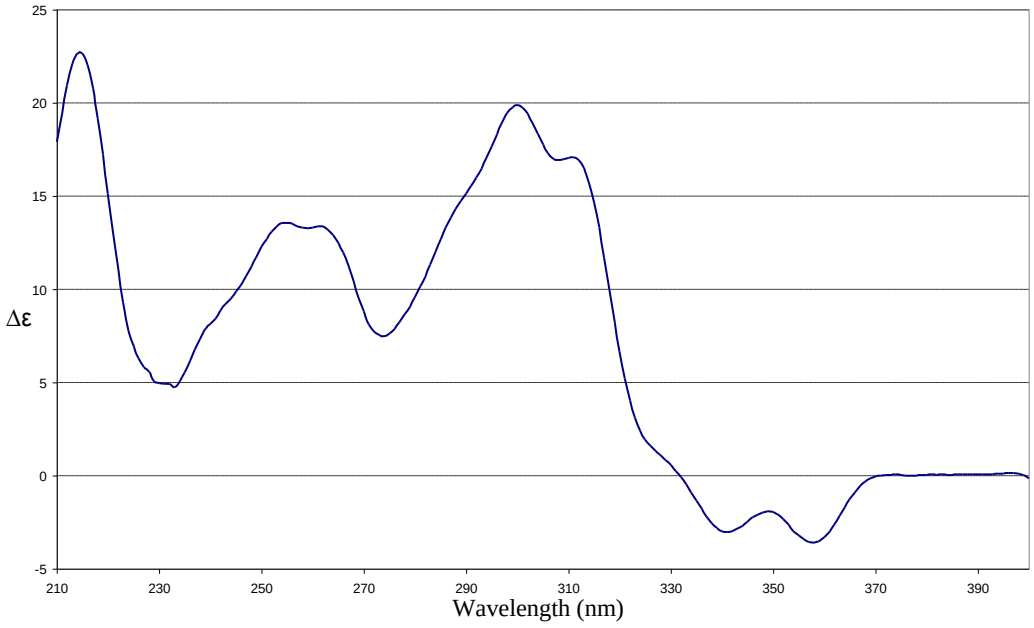

Figure S17. Circular dichroism spectrum for **1** obtained in methanol (22 ºC).

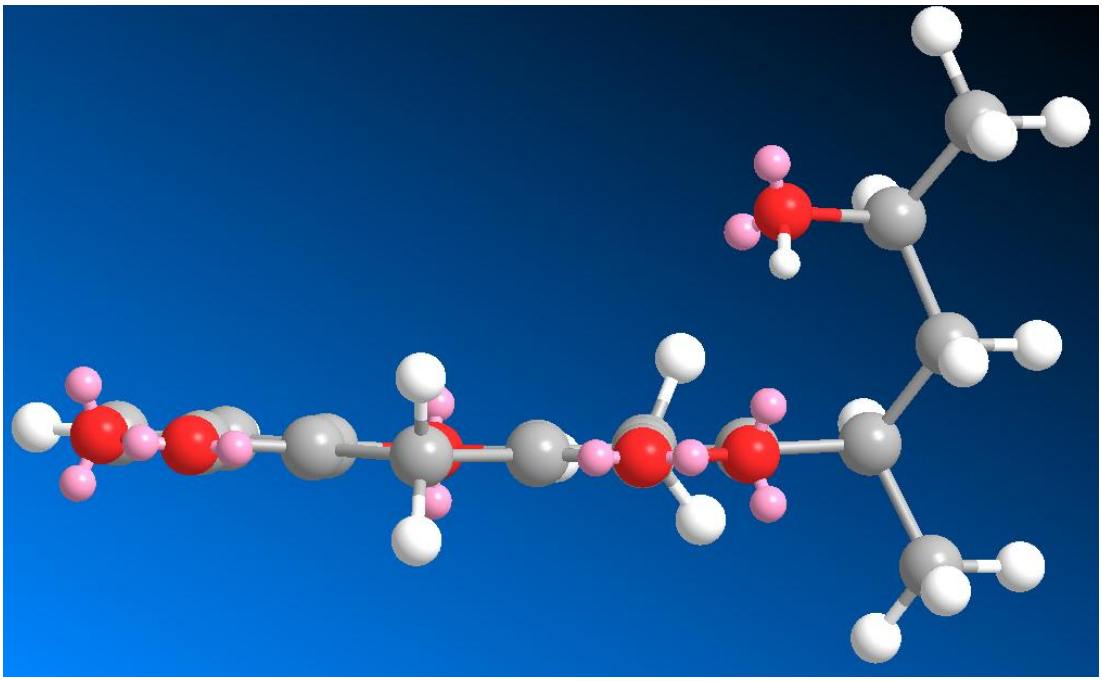

Figure S18A. Molecular model showing conformation of the side chain in **1** bearing (1′*R*,3′*S*)-configuration. The NOESY spectrum of **1** (Figure S12)confirms the shown orientation of the aromatic methyl and the proton attached to side-chain carbon 1'. Therefore, the negative Cotton effect (Figure S17) therefore requires (1'*R*)-configuration (compare Figure S18B).

Figure S18B. Molecular model showing conformation of the side chain in a hypothetical stereoisomer of **1** bearing (1′*S*,3′*S*)-configuration.

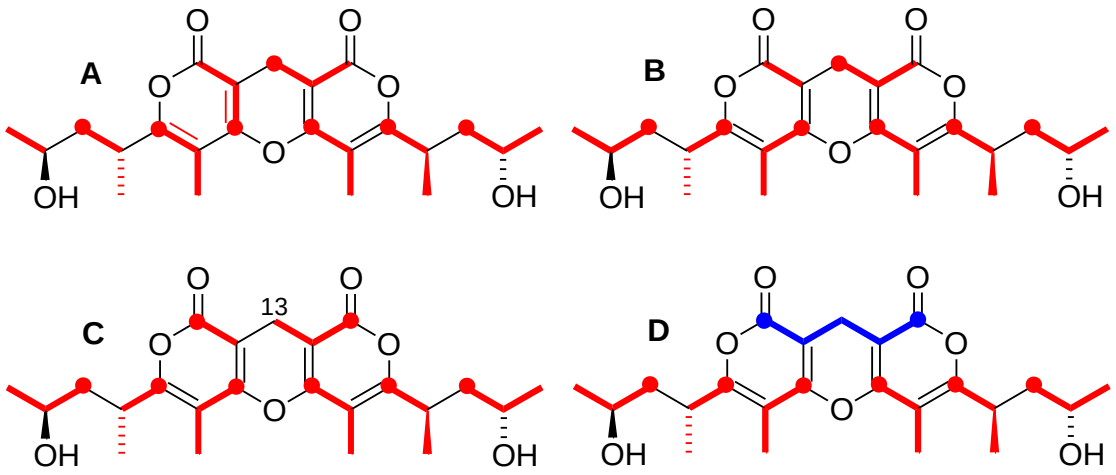

Figure S19. Models for the biosynthesis of **1**, from one contiguous polyketide chain derived from 8 units of propionate/methylmalonate followed by decarboxylation (**A**), from two similar or identical tetrapropionate units followed by decarboxylation (**B**), from two mixed acetate/propionate-derived polyketide chains (**C**), or two identical tripropionate units and one 5-carbon unit (blue) (**D**). Acetate and propionate-derived building blocks are shown in red. In model **C**, bridgehead carbon 13 could be of a different source.

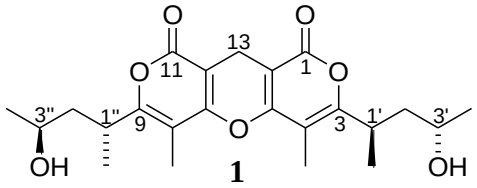

1

Table S2. NMR spectroscopic data in CD_3OD for catalipyrone A, **1** (HR-ESI$^+$MS *m/z* 419.206 (calcd for $C_{23}H_{31}O_7$ $[M+H]^+$ 419.2070); $[\alpha]_D^{20}$ = 165.8, *c* 1.05 in methanol).

Position	δ_H (mult., J_{HH})[a]	δ_C[b]	HMBC (H→C#)[a]	INADEQUATE[c]
1/11	---	165.0	---	12/14
3/9	---	164.5	---	4/8, 1′/1″
4/8	---	107.2	---	3/9, 5/7, 4-CH_3/8-CH_3
5/7	---	160.4	---	4/8, 12/14
12/14	---	99.7	---	5/7, 1/11, 13
13	3.24 (s)	18.1	1/11, 4[e]/8[e], 5/7, 12/14	12/14
1′/1″	3.36 (ddq, 4.1, 11, 6.9)[d]	32.4	3/9, 4/8, 2′/2″, 3′/3″, 1′-CH_3/1″-CH_3	3/9, 2′/2″, 1′-CH_3/1″-CH_3
2′/2″a	1.57 (ddd, 4.1,10, 14)	44.4	3/9, 1/1″, 3′/3″, 4’/4″, 1′-CH_3/1″-CH_3	1′/1″, 3′/3″
2′/2″b	1.87 (ddd, 2.9, 11, 14)	---	3/9, 1/1″, 3′/3″, 4’/4″, 1′-CH_3/1″-CH_3	---
3′/3″	3.50 (ddq, 2.9, 10, 6.2)[d]	66.1	1′/1″, 2′/2″, 4′/4″	2′/2″, 4′/4″
4’/4″	1.15 (d, 6.2)	24.2	2′/2″, 3′/3″	3′/3″
4-CH_3/8-CH_3	2.12 (s)	9.1	3/9, 4/8, 5/7	4/8
1′-CH_3/1″-CH_3	1.23 (d, 6.9)	19.1	3/9, 1′/1″, 2′/2″	1′/1″

[a] Recorded at 600 MHz. [b] Recorded at 125 MHz. [c] Recorded at 125 MHz. [d] Coupling constants determined by analysis of dqfCOSY cross-peaks. [e] Weak four-bond correlation.

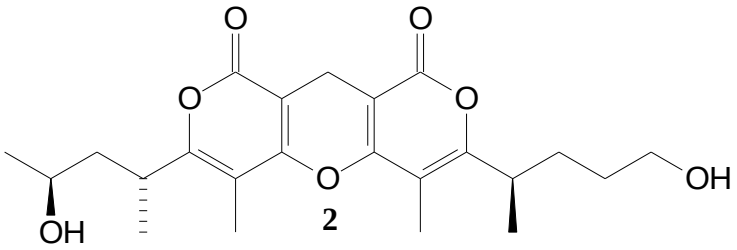

2

Table S3. NMR spectroscopic data in CD_3OD for catalipyrone B, **2** (HR-ESI$^+$MS *m/*z 419.206 (calcd for $C_{23}H_{31}O_7$ $[M+H]^+$ 419.2070); $[\alpha]_D^{20}$ = 99.5, *c* 1.05 in methanol).

Position	δ_H (mult., J_{HH})[a]	δ_C[b]	HMBC (H→C#)[a]
1	---	165.0[c]	---
3	---	164.5	---
4	---	107.3	---
5	---	160.5[d]	---
7	---	160.5[d]	---
8	---	106.8	---
9	---	164.9	---
11	---	165.0[c]	---
12	---	99.8[e]	---
13	3.24 (s)	18.1	1, 4[g], 5, 7, 8[g], 11, 12, 14
14	---	99.8[e]	---
1′	3.37 (ddq, 4.2, 11, 6.8)[f]	32.4	3, 4, 2′, 3′, 1′-CH_3
2′a	1.58 (ddd, 4.2, 10, 14)	44.4	3, 1′, 3′, 4′, 1′-CH_3
2′b	1.87 (ddd, 2.9, 11, 14)	---	3, 1′, 3′, 4′, 1′-CH_3
3′	3.50 (ddq, 2.9, 10, 6.2)	66.1	1′, 2′, 4′
4′	1.15 (d, 6.2)	24.3	2′, 3′
1″	3.10 (ddq,5.9, 9.0, 6.7)[f]	35.4	8, 9, 2″, 3″, 1″-CH_3
2″a	1.65 (dddd, 4.6, 5.9, 10, 14)[f]	31.8	9, 1″, 3″, 4″, 1″-CH_3
2″b	1.75 (dddd, 5.2, 9.0, 10, 14)[f]	---	9, 1″, 3″, 4″, 1″-CH_3
3″a	1.45 (dddt, 5.2, 10, 19, 6.5)[f]	31.2	1″, 2″, 4″
3″b	1.52 (dddt, 4.6, 10, 19, 6.5)[f]	---	1″, 2″, 4″
4″	3.54 (t, 6.5)	62.5	2″, 3″
4-CH_3	2.12 (s)	9.1	3, 4, 5
8- CH_3	2.10 (s)	9.1	7, 8, 9
1′- CH_3	1.24 (d, 6.8)	19.0	3, 1′, 2′
1″- CH_3	1.25 (d, 6.7)	18.4	9, 1″, 2″

[a] Recorded at 600 MHz. [b] Determined from HSQC and HMBC correlations. [c, d, e] These two carbons could not be distinguished. [f] Coupling constants determined by analysis of dqfCOSY cross-peaks. [g] Weak four-bond correlation.

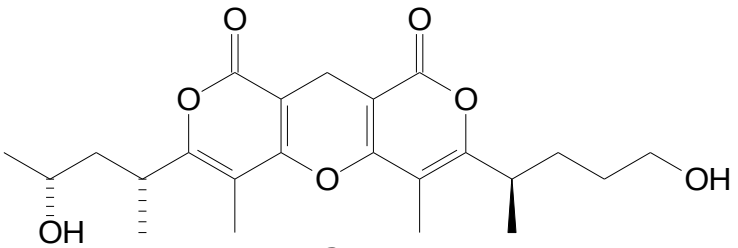

3

Table S4. NMR spectroscopic data in CD_3OD for catalipyrone C, **3** (HR-ESI$^+$MS *m/z* 419.206 (calcd for $C_{23}H_{31}O_7$ $[M+H]^+$ 419.2070); $[\alpha]_D^{20}$ = 113.5, *c* 1.09 in methanol).

Position	δ_H (mult., J_{HH})[a]	δ_C[b]	HMBC (H→C#)[a]
1	---	164.8[c]	---
3	---	165.6	---
4	---	105.6	---
5	---	160.5	---
7	---	160.4	---
8	---	106.7	---
9	---	164.7	---
11	---	164.8[c]	---
12	---	99.5[d]	---
13	3.23 (s)	18.1	1, 4[f], 5, 7, 8[f], 11, 12, 14
14	---	99.5[d]	---
1′	3.25 (ddq, 6.3, 8.2, 6.8)[e]	32.5	3, 4, 2′, 3′, 1′-CH_3
2′a	1.65 (ddd, 5.1, 8.2, 14)	44.2	3, 1′, 3′, 4′, 1′-CH_3
2′b	1.78 (ddd, 6.3, 8.9, 14)	---	3, 1′, 3′, 4′, 1′-CH_3
3′	3.77 (ddq, 5.1, 8.9, 6.2)	65.9	1′, 2′, 4′
4′	1.18 (d, 6.2)	23.8	2′, 3′
1″	3.10 (ddq, 6.4, 8.9, 6.8)[e]	35.5	8, 9, 2″, 3″, 1″-CH_3
2″a	1.65 (dddd, 5.1, 6.4, 10, 14)[e]	31.8	9, 1″, 3″, 4″, 1″-CH_3
2″b	1.74 (dddd, 4.4, 8.9, 10, 14)[e]	---	9, 1″, 3″, 4″, 1″-CH_3
3″a	1.45 (dddt, 4.4, 10, 19, 6.5)[e]	31.2	1″, 2″, 4″
3″b	1.52 (dddt, 5.1, 10, 19, 6.5)[e]	---	1″, 2″, 4″
4″	3.54 (t, 6.5)	62.4	2″, 3″
4-CH_3	2.10 (s)	9.0	3, 4, 5
8- CH_3	2.10 (s)	9.1	7, 8, 9
1′- CH_3	1.24 (d, 6.8)	17.7	3, 1′, 2′
1″- CH_3	1.25 (d, 6.8)	18.4	9, 1″, 2″

[a] Recorded at 600 MHz. [b] Determined from HSQC and HMBC correlations. [c, d] These two carbons could not be distinguished. [e] Coupling constants determined by analysis of dqfCOSY cross-peaks. [f] Weak four-bond correlation.

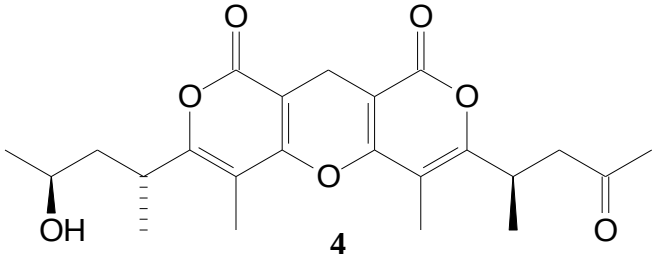

4

Table S5. NMR spectroscopic data in CD_3OD for catalipyrone D, **4** (HR-ESI$^+$MS *m/z* 417.192 (calcd for $C_{23}H_{29}O_7$ $[M+H]^+$ 417.1913)).

Position	δ_H (mult., J_{HH})[a]	δ_C[b]	HMBC (H→C#)[a]
1	---	164.9[c]	---
3	---	164.6	---
4	---	107.3	---
5	---	160.5	---
7	---	160.6	---
8	---	106.5	---
9	---	164.2	---
11	---	164.9[c]	---
12	---	99.8[d]	---
13	3.22 (s)	18.2	1, 4[e], 5, 7, 8[e], 11, 12, 14
14	---	99.8[d]	---
1′	3.36 (ddq, 4.2, 11, 6.9)	32.5	3, 4, 2′, 3′, 1′-CH_3
2′a	1.57 (ddd, 4.2, 10, 14)	44.5	3, 1′, 3′, 4′, 1′-CH_3
2′b	1.86 (ddd, 3.0, 11, 14)	---	3, 1′, 3′, 4′, 1′-CH_3
3′	3.50 (m)	66.1	1′, 2′, 4′
4′	1.15 (d, 6.2)	24.3	2′, 3′
1″	3.50 (m)	31.1	8, 9, 2″, 3″, 1″-CH_3
2″a	2.79 (dd, 5.4, 18)	47.7	9, 1″, 3″, 1″-CH_3
2″b	3.02 (dd, 8.9, 18)	---	9, 1″, 3″, 1″-CH_3
3″	---	208.8	---
4″	2.13 (s)	29.8	2″, 3″
4-CH_3	2.12 (s)	9.2	3, 4, 5
8- CH_3	2.14 (s)	9.1	7, 8, 9
1′- CH_3	1.23 (d, 6.9)	19.0	3, 1′, 2′
1″- CH_3	1.21 (d, 7.0)	18.4	9, 1″, 2″

[a] Recorded at 600 MHz. [b] Determined from HMBC correlations. [c, d] These two carbons could not be distinguished. [e] Weak four-bond correlation.

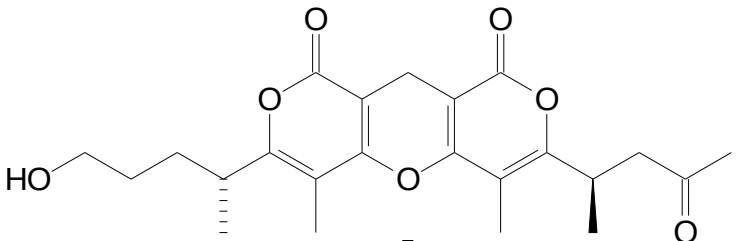

5

Table S6. NMR spectroscopic data in CD_3OD for catalipyrone E, **5** (HR-ESI$^+$MS *m/z* 417.192 (calcd for $C_{23}H_{29}O_7$ $[M+H]^+$ 417.1913)).

Position	δ_H (mult., J_{HH})[a]	δ_C[b]	HMBC (H→C#)[a]
1	---	164.8[c]	---
3	---	164.9	---
4	---	106.8	---
5	---	160.5	---
7	---	160.6	---
8	---	106.5	---
9	---	164.2	---
11	---	164.8[c]	---
12	---	99.7[d]	---
13	3.23 (s)	18.2	1, 4[e], 5, 7, 8[e], 11, 12, 14
14	---	99.7[d]	---
1′	3.10 (m)	35.5	3, 4, 2′, 3′, 1′-CH_3
2′a	1.64 (m)	31.9	3, 1′, 3′, 4′, 1′-CH_3
2′b	1.75 (m)	---	3, 1′, 3′, 4′, 1′-CH_3
3′a	1.45 (m)	31.2	1′, 2′, 4′
3′b	1.52 (m)	---	1′, 2′, 4′
4′	3.54 (t, 6.5)	62.5	2′, 3′
1″	3.50 (ddq, 5.3, 8.9, 7.0)	31.1	8, 9, 2″, 3″, 1″-CH_3
2″a	2.79 (dd, 5.3, 18)	47.7	9, 1″, 3″, 1″-CH_3
2″b	3.02 (dd, 8.9, 18)	---	9, 1″, 3″, 1″-CH_3
3″	---	208.7	---
4″	2.13 (s)	29.8	2″, 3″
4-CH_3	2.10 (s)	9.2	3, 4, 5
8- CH_3	2.14 (s)	9.0	7, 8, 9
1′- CH_3	1.25 (d, 6.8)	18.5	3, 1′, 2′
1″- CH_3	1.21 (d, 7.0)	18.4	9, 1″, 2″

[a] Recorded at 600 MHz. [b] Determined from HMBC correlations. [c, d] These two carbons could not be distinguished. [e] Weak four-bond correlation.

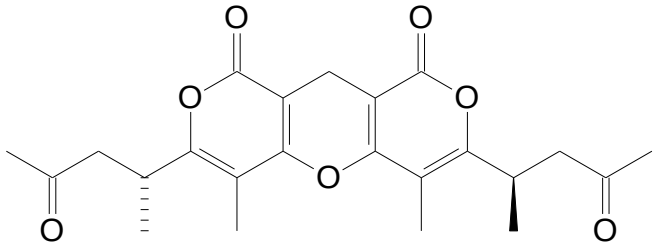

6

Table S7. NMR spectroscopic data in CD_3OD for catalipyrone F, **6** (HR-ESI$^+$MS *m/z* 415.174 (calcd for $C_{23}H_{27}O_7$ $[M+H]^+$ 415.1757)).

Position	δ_H (mult., J_{HH})[a]	δ_C[b]	HMBC (H→C#)[a]
1/11	---	164.8	---
3/9	---	164.3	---
4/8	---	106.6	---
5/7	---	160.6	---
12/14	---	99.7	---
13	3.21 (s)	18.2	1/11, 4[c]/8[c], 5/7, 12/14
1′/1″	3.50 (ddq, 5.2, 8.8, 7.0)	31.1	2′/2″, 3′/3″, 1′-CH_3/1″-CH_3
2′/2″a	2.79 (dd, 5.2, 18)	47.8	3/9, 1′/1″, 3′/3″, 1′-CH_3/1″-CH_3
2′/2″b	3.02 (dd, 8.8, 18)	---	3/9, 1′/1″, 3′/3″, 1′-CH_3/1″-CH_3
3′/3″	---	208.9	---
4′/4″	2.13 (s)	29.8	2′/2″, 3′/3″
4-CH_3/8-CH_3	2.14 (s)	9.1	3/9, 4/8, 5/7
1′-CH_3/1″-CH_3	1.21 (d, 7.0)	18.5	3/9, 1′/1″, 2′/2″

[a] Recorded at 600 MHz. [b] Determined from HMBC correlations. [c] Weak four-bond correlation.

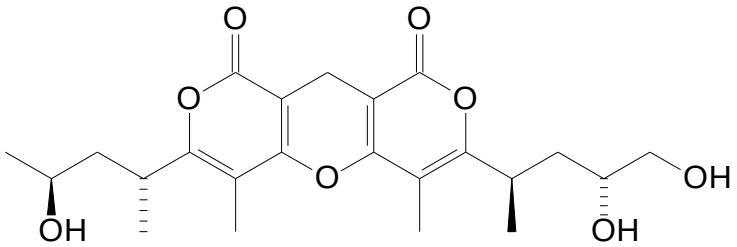

7

Table S8. NMR spectroscopic data in CD_3OD for catalipyrone G, 7 (HR-ESI$^+$MS *m/z* 435.204 (calcd for $C_{23}H_{31}O_8$ $[M+H]^+$ 435.2019)).

Position	δ_H (mult., J_{HH})[a]	δ_C[b]	HMBC (H→C#)[a]
1	---	164.9[c]	---
3	---	164.5	---
4	---	107.1	---
5	---	160.4	---
7	---	160.2	---
8	---	107.3	---
9	---	164.2	---
11	---	164.9[c]	---
12	---	99.6[d]	---
13	3.24 (s)	18.1	1, 5, 7, 11, 12, 14
14	---	99.6[d]	---
1′	3.37 (ddq, 4.3, 11, 7.0)[e]	32.4	[f]
2′a	1.57 (ddd, 4.3, 10, 14)[e]	44.3	3, 1′, 3′, 4′, 1′-CH_3
2′b	1.87 (ddd, 2.9, 11, 14)[e]	---	[f]
3′	3.49 (ddq, 2.9, 10, 6.1)[e]	66.0	[f]
4′	1.15 (d, 6.1)	24.2	2′, 3′
1″	3.41 (ddq, 4.1, 11, 7.0)[e]	32.0	[f]
2″a	1.55 (ddd, 4.1, 11, 14)[e]	38.8	9, 1″, 3″, 1″-CH_3
2″b	1.94 (ddd, 2.5, 11, 14)[e]	---	[f]
3″	3.32 (ddt, 2.5, 11, 5.5)[e]	70.8	[f]
4″	3.41 (d, 5.5)	67.5	2″, 3″
4-CH_3	2.13 (s)	9.1	3, 4, 5
8-CH_3	2.14 (s)	9.2	7, 8, 9
1′-CH_3	1.24 (d, 7.0)	19.0	3, 1′, 2′
1″-CH_3	1.26 (d, 7.0)	19.1	9, 1″, 2″

[a] Recorded at 600 MHz. [b] Determined from HSQC and HMBC correlations. [c, d] These two carbons could not be distinguished. [e] Coupling constants determined by analysis of dqfCOSY cross-peaks. [f] No signals observed.

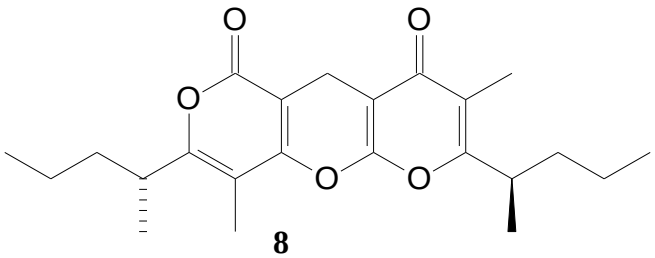

8

Table S9. NMR spectroscopic data in acetone-d_6 for catalipyrone H, **8** (HR-ESI$^+$MS *m/*z 387.217 (calcd for $C_{23}H_{31}O_5$ $[M+H]^+$ 387.2172)).

Position	δ_H (mult., J_{HH})[a]	δ_C[b]	HMBC (H→C#)[a]
2	---	163.6	---
3	---	119.2	---
4	---	180.1	---
5	---	100.5	---
6	3.24 (s)	18.3	4, 5, 7, 8, 12, 14
7	---	97.9	---
8	---	163.7	---
10	---	164.4	---
11	---	104.4	---
12	---	159.5	---
14	---	159.3	---
1′	3.08 (ddq, 8.8, 12, 6.8)[c]	34.8	2′, 3′, 1′-CH_3
2′a	1.51 (m)	36.9	10, 1′, 3′, 4′, 1′-CH_3
2′b	1.68 (m)	---	10, 1′, 3′, 4′, 1′-CH_3
3′	1.26 (m)	21.8	4′
4′	0.91 (t, 7.5)	14.1	2′, 3′
1″	3.15 (ddq, 8.8, 12, 6.9)[c]	35.1	2″, 3″, 1″-CH_3
2″a	1.53 (m)	36.8	2, 1″, 3″, 4″, 1″-CH_3
2″b	1.69 (m)	---	2, 1″, 3″, 4″, 1″-CH_3
3″	1.31 (m)	21.7	4″
4″	0.92 (t, 7.3)	14.0	2″, 3″
3-CH_3	1.95 (s)	9.4	2, 3, 4
11-CH_3	2.02 (s)	8.9	10, 11, 12
1′-CH_3	1.22 (d, 6.8)	18.3	10, 1′, 2′
1″-CH_3	1.25 (d, 6.9)	18.2	2, 1″, 2″

[a] Recorded at 600 MHz. [b] Determined from HMQC and HMBC correlations. [c] Coupling constants determined by analysis of dqfCOSY cross-peaks.

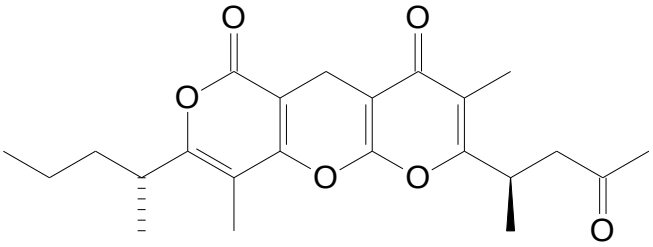

9

Table S10. NMR spectroscopic data in acetone-d_6 for catalipyrone I, **9** (HR-ESI$^+$MS *m/z* 401.196 (calcd for $C_{23}H_{29}O_6$ $[M+H]^+$ 401.1964)).

Position	δ_H (mult., J_{HH})[a]	δ_C[b]	HMBC (H→C#)[a]
2	---	163.1	---
3	---	118.9	---
4	---	178.8	---
5	---	100.3	---
6	3.22 (s)	18.4	4, 5, 7, 8, 12, 14
7	---	97.1	---
8	---	162.5	---
10	---	164.3	---
11	---	104.7	---
12	---	159.1	---
14	---	159.0	---
1′	3.08 (m)	35.0	[d]
2′a	1.50 (m)	37.4	[d]
2′b	1.65 (m)	---	[d]
3′	1.28 (m)	21.1	[d]
4′	0.89 (t, 7.3)	14.1	2′, 3′
1″	3.56 (ddq, 6.4, 7.2, 6.9)[c]	30.9	[d]
2″a	3.01 (dd, 7.9, 18)	47.1	1″, 3″, 1″-CH_3
2″b	2.85 (dd, 5.7, 18)[c]	---	2, 1″, 3″, 1″-CH_3
3″	---	206.0	---
4″	2.12 (s)	29.7	2″, 3″
3-CH_3	1.97 (s)	9.3	2, 3, 4
11-CH_3	2.06 (s)	9.0	10, 11, 12
1′-CH_3	1.19 (d, 6.9)	18.3	10, 1′, 2′
1″-CH_3	1.24 (d, 6.9)	17.9	2, 1″, 2″

[a] Recorded at 600 MHz. [b] Determined from HMQC and HMBC correlations. [c] Coupling constants determined by analysis of dqfCOSY cross-peaks. [d] No signals observed.

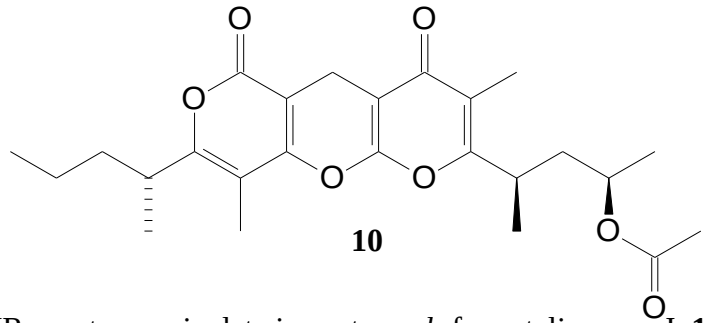

10

Table S11. NMR spectroscopic data in acetone-d_6 for catalipyrone J, **10** (HR-ESI$^+$MS *m/*z 445.220 (calcd for $C_{25}H_{33}O_7$ $[M+H]^+$ 445.2226)).

Position	δ_H (mult., J_{HH})[a]	δ_C[b]	HMBC (H→C#)[a]
2	---	163.4	---
3	---	118.7	---
4	---	178.7	---
5	---	100.2	---
6	3.24 (s)	18.4	4, 5, 7, 8, 12, 14
7	---	97.0	---
8	---	161.7	---
10	---	164.2	---
11	---	104.7	---
12	---	159.2	---
14	---	159.0	---
1′	3.08 (m)	34.9	[d]
2′a	1.50 (m)	37.2	[d]
2′b	1.65 (m)	---	[d]
3′	1.29 (m)	21.0	[d]
4′	0.90 (t, 7.4)	14.1	2′, 3′
1″	3.23 (ddq, 6.6, 8.5, 6.9)[c]	32.9	[d]
2″a	1.79 (ddd, 4.0, 6.6, 14)[c]	40.4	[d]
2″b	2.06 (ddd, 8.5, 9.5, 14)[c]	---	[d]
3″	4.95 (ddq, 4.0, 9.5, 6.3)[c]	69.5	[d]
4″	1.21 (d, 6.3)	20.5	2″, 3″
3-CH_3	1.92 (s)	9.3	2, 3, 4
11-CH_3	2.06 (s)	8.9	10, 11, 12
1′-CH_3	1.19 (d, 6.8)	18.3	10, 1′, 2′
1″-CH_3	1.27 (d, 6.9)	18.3	2, 1″, 2″
1‴	---	170.3	---
2‴	1.87 (s)	22.6	1‴

[a] Recorded at 600 MHz. [b] Determined from HMQC and HMBC correlations. [c] Coupling constants determined by analysis of dqfCOSY cross-peaks. [d] No signals observed.

References

1. Claridge TDW (2009) in *High-Resolution NMR Techniques in Organic Chemistry* (Elsevier), pp 35-98.
2. Claridge TDW (2009) in *High-Resolution NMR Techniques in Organic Chemistry* (Elsevier), pp 129-188.
3. Severson RF, *et al.* (1984) Quantitation of the Major Cuticular Components from Green Leaf of Different Tobacco Types. *J Agric Food Chem* 32:566-570.
4. Himmelsbach DS, van Halbeek H, Arrendale RF, Severson RF (1990) Assignment of proton and carbon-13 spectra of a sucrose ester from tobacco by inverse detected two-dimensional heteronuclear correlated NMR spectroscopy. *Magn Reson Chem* 28:682-687.
5. Cutignano A, Fontana A, Renzulli L, Cimino G (2003) Placidines C-F, Novel a-Pyrone Propionates from the Mediterranean Sacoglossan Placia dendritica. *J Nat Prod* 66:1399-1401.
6. Forster PG, Ghisalberti EL, Jefferies PR (1987) A New Class of Monocyclic Diterpenes from Eremophila foliosissima Kraenzlin. (Myoporaceae). *Tetrahedron* 43:2999-3007.
7. Brown JM, Naik RG (1982) Chelate Control in the Rhodium-catalysed Homogeneous Hydrogenation of Chiral Allylic and Homoallylic Alcohols. *J Chem Soc, Chem Commun*:348-350.